

Supplementary Materials for **Time scale bias in erosion rates of glaciated landscapes**

Vamsi Ganti, Christoph von Hagke, Dirk Scherler, Michael P. Lamb, Woodward W. Fischer,
Jean-Philippe Avouac

Published 5 October 2016, *Sci. Adv.* **2**, e1600204 (2016)
DOI: 10.1126/sciadv.1600204

This PDF file includes:

- Supplementary Materials and Methods
- fig. S1. Effect of heavy-tailed erosional hiatuses on estimated erosion rates.
- fig. S2. Illustration of the effect of heavy-tailed erosional hiatuses on overshadowing a systematic increase in magnitudes of erosional pulses with age.
- fig. S3. Cumulative erosion versus averaging time scale for glaciated and fluvial landscapes.
- fig. S4. Numerical simulations highlighting the effect of varying magnitudes of erosional pulses.
- fig. S5. Location maps of data for fluvial landscapes.
- fig. S6. Location maps of data for glaciated landscapes.
- table S1. Landscape setting and fitted scaling exponents.
- table S2. Tabulated data used in this study.
- References (87–130)

Supplementary Materials and Methods

Supplementary Note 1: Erosional hiatuses and their effect on estimates of erosion rates

Consider a time series of erosion over million year time scales (Fig. 1). The estimated erosion rate (E_{obs}) represents a running average of the time series over a given averaging time scale T , that is,

$$E_{obs}(T) = \frac{\sum_{i=1}^n Y_i}{T} \quad (1)$$

where Y_i denotes the magnitudes of erosional pulses, n represents the number of erosional pulses sampled during a given averaging time scale T . Because most geochronological methods average magnitudes of erosional pulses and hiatuses from some time in the past to the present, the averaging time scale T and age are correlated and this denotes the time scale accessed by a given method. For example, T would represent decadal scales for erosion rates estimated from sediment yield data and it would represent millennial scales for erosion rates estimated from cosmogenic nuclides. The estimated erosion rate reflects both the erosional pulses and hiatuses. See *Schumer and Jerolmack (10)* for a detailed discussion of the effect of hiatuses on estimated rates of landscape change in the context of sedimentation rates.

In probability theory, the law of large numbers describes the long-term stability of the mean of a sequence of random numbers. If the erosional hiatuses have a distribution with a finite mean (thin-tailed, e.g., exponential), then the sample mean converges to the mean of pulses of erosion, which is normalized by the mean of the erosional hiatuses (*10, 87*). However, if the erosional hiatuses have a heavy-tailed distribution with an infinite mean (e.g., Pareto), then the sample mean need not converge to a constant value (*10*). Heavy-tailed distributions are characterized by power-law decay in the tails of their cumulative distribution function ($t^{-\alpha}$) and these distributions have infinite means when $\alpha < 1$. Heavy-tailed distributions assign a small but finite chance for the occurrence of extremely large events (in this case erosional hiatuses). In contrast, for thin-tailed random variables, the chance of occurrence of extreme events is effectively zero. When the erosional hiatuses have a heavy-tailed distribution with an infinite mean, then estimated erosion rates exhibit inverse power-law dependence on the averaging time scale where the scaling exponent is given by $\alpha < 1$ (see (*10*) for a detailed derivation). If the erosional hiatuses have an upper bound then the distribution is truncated and the time scale bias in estimated erosion rates ceases to exist beyond averaging time scales that approach the longest plausible hiatus, and erosion rates measured over time scales longer than the upper bound of the distribution of erosional hiatuses will represent mean rates of erosional pulses (*10, 14*), which are normalized by the mean of the truncated heavy-tailed distribution of erosional hiatuses.

We performed numerical simulations that demonstrate the aforementioned concepts with results shown in fig. S1. In this example, for simplicity, we ignored the variability in magnitudes of erosional pulses and assume that each erosional pulse represents 10 mm of erosion and these erosional pulses are interspersed among erosional hiatuses (e.g., fig. S1). We sampled the erosional hiatuses from three different distributions: (a) exponential distribution (mean of 100 years), (b) Pareto distribution ($\alpha = 0.5$; no finite mean), and (c) truncated Pareto distribution (mean of 225 years). These three distributions represent a thin-tailed distribution, heavy-tailed distribution, and a heavy-tailed distribution with an upper bound, respectively. In the first case, the representative erosion rate for the catchment is the magnitude of erosion during each year (10 mm) divided by the average time interval between erosional pulses (mean of 100 years), which is 0.1 mm/year. In the second case, there is no representative mean erosional hiatus as the distribution of erosional hiatuses is heavy-tailed with a tail index less than 1. Finally, in the third case, the representative erosion rate for the catchment is the magnitude of erosional

pulses during each year (10 mm) divided by the average time interval between erosional pulses (mean of 225 years), which is 0.045 mm/year.

The estimated erosion rates from the simulated time series of erosion demonstrate the aforementioned theory: for the case that erosional hiatuses have a thin-tailed distribution (in this case an exponential distribution; gray markers in fig. S1), the running average of the time series of erosional pulses converge to a value of 0.1 mm/year. In contrast, the estimated erosion rates show an inverse power-law trend with averaging time scale with a scaling exponent of $\alpha - 1$ when the distribution of erosional hiatuses has a heavy tail with tail index α (red markers in fig. S1). Further, when the erosional hiatuses have a heavy-tailed distribution with an upper bound, the estimated erosion rates converge to a value of 0.045 mm/year for averaging time scales longer than the upper bound of the erosional hiatuses (blue markers in fig. S1 similar to results shown in Fig. 4C). We note that magnitudes of erosional pulses can themselves be variable; however, heavy-tailed magnitudes of erosional pulses with an infinite mean will result in a positive power-law trend in the averaging time scale dependence of estimated erosion rates (opposite trend to that observed in Fig. 2A, and a trend reported by (17)). These scaling relationships do not change if the magnitudes of erosional pulses were variable but drawn from a thin-tailed distribution (10) (e.g., exponential distribution).

We can visualize the effect of averaging time scale dependence of estimated erosion rates on overshadowing the systematic increase in magnitudes of erosional pulses with age as shown in fig. S2. We generated 1000 independent time series of erosional pulses of equal magnitude (10 mm) interspersed with erosional hiatuses (truncated Pareto, tail index = 0.5; upper bound = 200 ky) and computed erosion rates for different averaging time scales (10^2 years and 10^4 years) with age using a window average filter. We then computed the slope and intercept of the best fitting power law that describes the functional dependence of erosion rate on age (and not averaging time scale). The blue and red lines in fig. S2 indicate the relation between erosion rate and age for averaging time scales of 10^2 years and 10^4 years, respectively, where a 10-fold difference between estimated erosion rates is evident with different averaging time scale over all ages. Thus, only changes in magnitudes of erosional pulses that are greater than 10-fold can overshadow the dominant signature of heavy-tailed erosional hiatuses on averaging time scale.

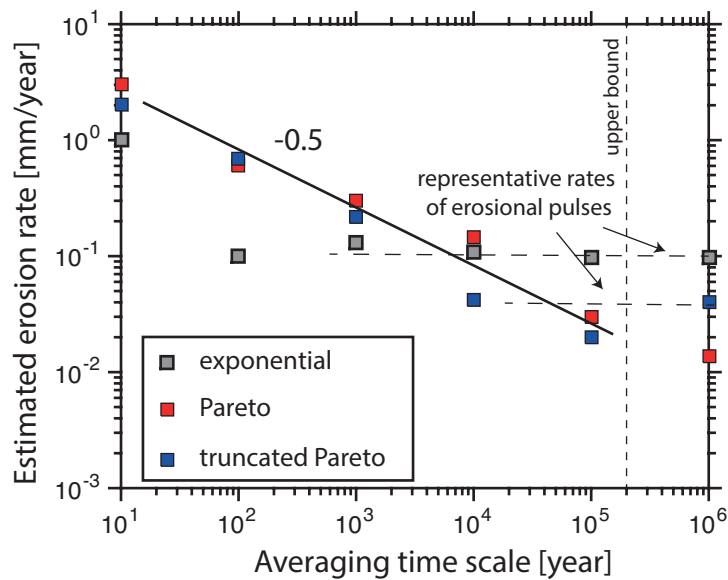


fig. S1. Effect of heavy-tailed erosional hiatuses on estimated erosion rates. Plot showing results of time scale bias in estimated erosion rates from numerical simulations where the magnitudes of erosional pulses were constant through time (10 mm) and the distribution of erosional hiatuses were changed. In these simulations the estimated erosion rates average from some time in the past to the present, such that the averaging time scale is equal to the age. Time scale bias in estimated erosion rates for the case of thin-tailed erosional hiatuses (exponentially distributed, gray markers) significantly differs from the cases when erosional hiatuses are heavy tailed with (truncated Pareto distribution; blue markers) and without an upper bound (Pareto distribution; red markers). The tail index for both these heavy-tailed erosional hiatuses was 0.5. The different representative rates of erosional pulses are a result of the different means of erosional hiatuses and the vertical dashed line indicates the upper bound on the erosional hiatuses with a truncated Pareto distribution.

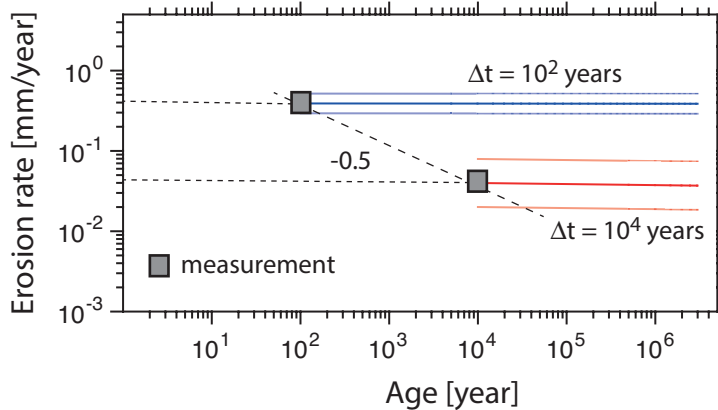


fig. S2. Illustration of the effect of heavy-tailed erosional hiatuses on overshadowing the systematic increase in magnitudes of erosional pulses with age. Erosion rate as a function of age for different averaging time scales (blue line is $\Delta t = 10^2$ years, and red line is $\Delta t = 10^4$ years). The estimated erosion rate shows approximately a 10-fold decrease for all ages with a 100-fold increase in averaging time scale. The opaque and translucent lines of the same color show the best fitting power law functions with mean power-law slope and intercept along with their standard error (SE) evaluated by averaging over 1000 different realizations.

Supplementary Note 2: Dependence of cumulative erosion on averaging time scale

Previous work argued that plotting erosion rate versus averaging time scale could lead to spurious correlations because time features in both the independent and the dependent variables (45). The power-law exponents reported in Fig. 2 are directly related to the power-law exponents on the relation describing the dependence of cumulative erosion on averaging time scale. Here, we provide additional plots of cumulative erosion versus averaging time scale for all glaciated and fluvial landscapes from our compilation. Both these plots demonstrate that the power-law exponents reported in Fig. 2 are directly transformable into power-law exponents that describe the averaging time scale dependence of cumulative erosion, where exponent on the length-time plot (fig. S3) is the result of adding 1 to the rate-time plot (Fig. 2). In both these plots, cumulative erosion for thermochronological systems was derived from their respective closure temperatures by assuming a geothermal gradient of 30°C/km. For cosmogenic nuclide derived erosion rates, we assign the cumulative erosion to be 60 cm.

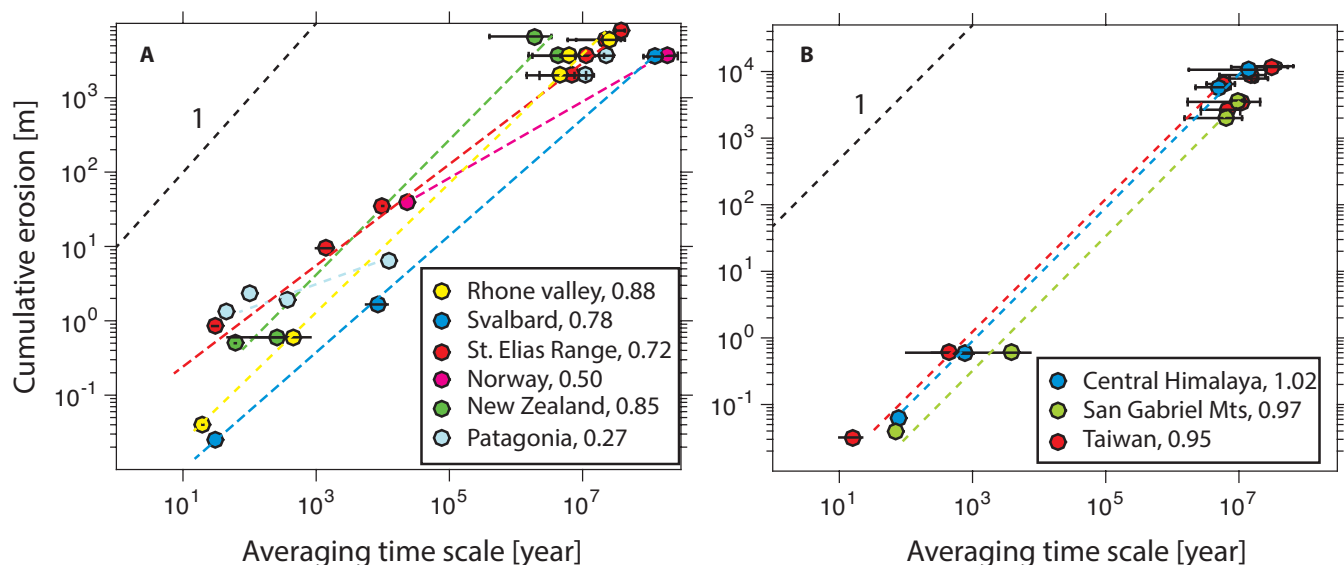


fig. S3. Cumulative erosion versus averaging time scale for glaciated and fluvial landscapes. (A, B) Cumulative erosion versus averaging time scale for all glaciated and fluvial landscapes where the depth of erosion for cosmogenic nuclide data was assigned to be 60 cm and the depth of erosion for thermochronometers were derived from geothermal gradient and closure temperature. Erosion rates derived from sediment yield and fjord sedimentation were converted to a depth of erosion by multiplying the estimated erosion rate and the averaging time scale. The slope of the power-law scaling is directly related to the slope of the power-law reported in Fig. 2 where the scaling of the rate-time plot can be transformed to scaling of the length-time plot by adding 1 (45). The dashed black line indicates a slope of 1, which is expected if the erosion rate was constant through time. The number in the legend indicates the slope of the best-fitting power-law that describes the dependence of cumulative erosion on averaging time scale for each landscape.

Supplementary Note 3: Effect of varying magnitudes of erosional pulses

In the main text, we have shown numerical simulations with variable duration of erosional hiatuses and constant magnitudes of erosional pulses. To assess whether variable magnitudes of erosional pulses can affect the time scale bias in estimated erosion rates, we performed numerical simulations to test theoretical expectations. Theoretical expectations suggest that negative power-law dependence of erosion rates on averaging time scale can only result from heavy-tailed erosional hiatuses with a tail

index less than 1 (10). To assess if varying magnitudes of erosional pulses can affect this trend, we relaxed the assumption of constant magnitudes of erosional pulses that was imposed in the numerical simulations presented in the main text. Instead, we generated time series of landscape scale erosion with the difference that the magnitudes of erosional pulses were variable. We sampled magnitudes of erosional pulses from a thin-tailed distribution (fig. S4A; exponential distribution with a mean of 10 mm for 0-1 My and a mean that was two and ten times lower for time greater than 1 My) and a heavy-tailed distribution (fig. S4C; Pareto distribution with a scale parameter of 10 mm and tail index of 1.5). The erosional hiatuses had the same distribution and structure, that is, drawn from a truncated Pareto distribution with tail index of 0.5 and upper bound of 200 ky. The results highlight that the time scale bias in estimated erosion rates is still dominated by the heavy-tailed erosional hiatuses where the power-law slope is equal to -0.5 , thereby confirming theoretical expectations that the negative power-law scaling of estimated erosion rates on averaging time scale arises from heavy-tailed erosional hiatuses and is unaffected by varying magnitudes of erosional pulses.

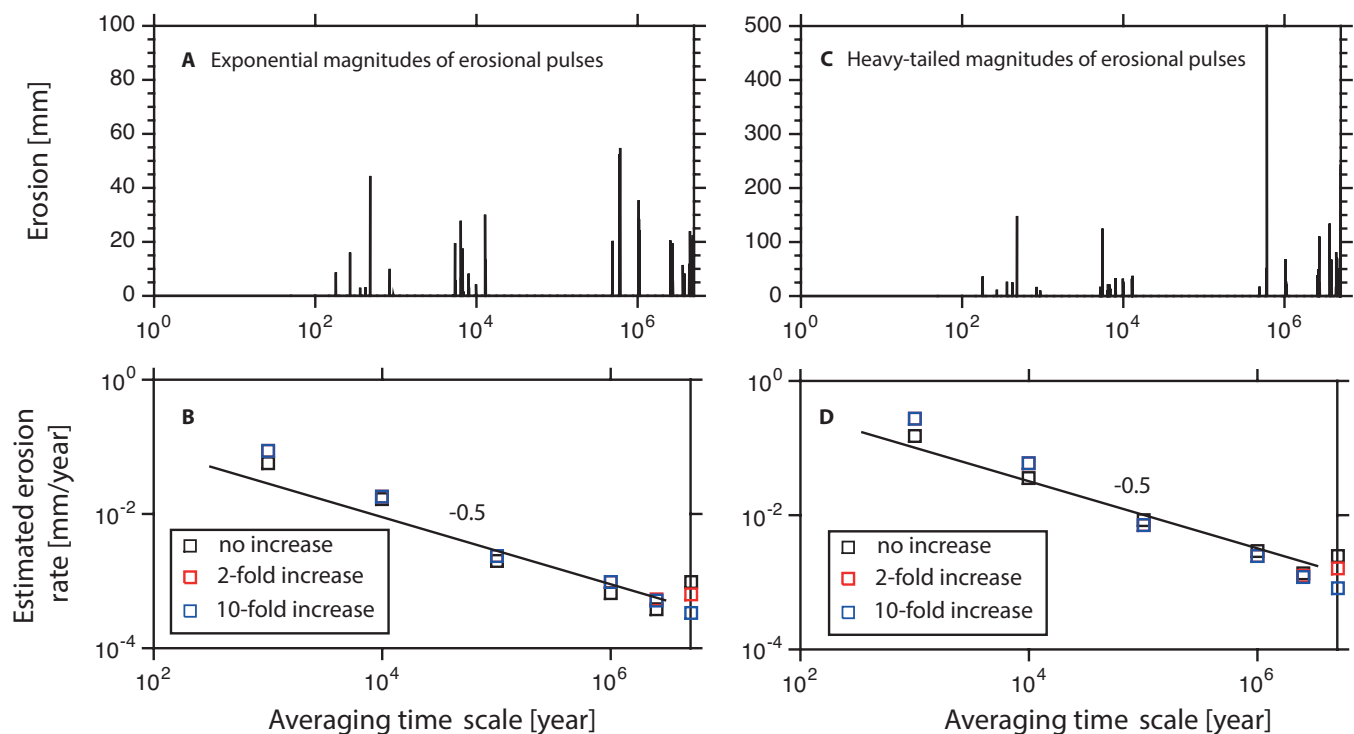


fig. S4. Numerical simulations highlighting the effect of varying magnitudes of erosional pulses. (A, C) In both these simulations, we had the same probabilistic structure of erosional hiatuses, i.e., truncated Pareto distribution with tail index 0.5 and upper bound 200 ky; however, we chose the magnitudes of erosional pulses from an exponential distribution and Pareto distribution, respectively. The mean magnitudes of erosional pulses were two (red markers) and ten times (blue markers) higher for 0-1 My when compared to magnitudes of erosional pulses for time greater than 1 My. The black markers are results from simulations with no change in the statistics of magnitudes of erosional pulses through time. (B, D) The averaging time scale dependence of estimated erosion rates is dominated by heavy-tailed erosional hiatuses confirming theoretical expectations (10). In these simulations the estimated erosion rates average from some time in the past to the present, such that the averaging time scale is equal to the age.

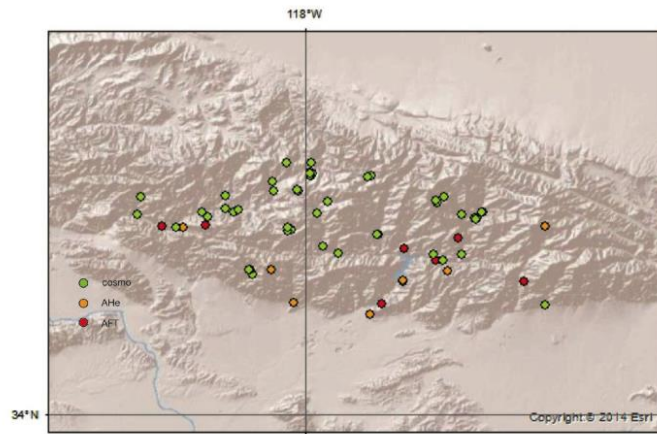
Supplementary Note 4

In some of the landscapes there is spatial variability in the compiled data set, which has to be accounted for when comparing erosion rate estimates. In particular, in New Zealand the distance to the Alpine Fault has been shown to have significant influence on cooling ages. Erosion rates are not highest at the Alpine Fault itself, but approximately 5 – 7 km south of it (88). Our data compilation spans the entire region of very high erosion rates only, not extending into the reaches farther south, where a strong decline in erosion rates is observed. Additionally, cosmogenic nuclide ages and sediment yield data are catchment-averaged erosion rates and compiled for the same area, and are thus comparable to the averaged in situ measurements within the catchment.

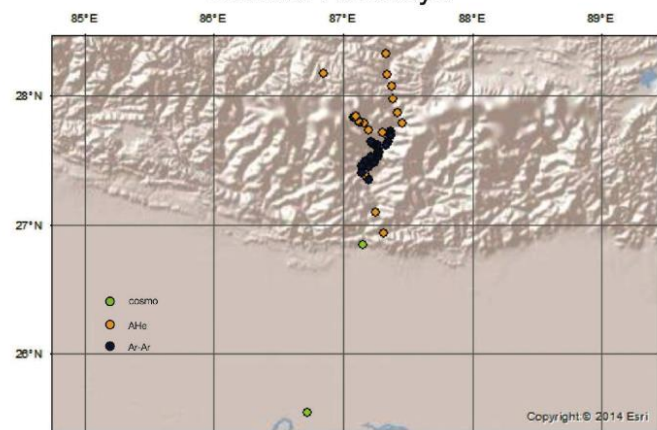
In Taiwan, an extensive study showed variability of sediment yield data (89). Some of these measurements are higher than the long-term average, which is represented within the error bars of our compilation. The European Alps have been argued to be at steady state based on thermochronological data (90, 91). However, these data may not be sensitive to the influence of the last glaciation, given the large response time of the system (92), and the youngest history including glaciation may not be resolved (90). Furthermore, the Alps are heavily effected by human activity, which may have an impact on measured sediment yield data (93).

We classified the central Himalayas as a fluvial landscape for the following reasons. In the sub-tropical region of the central Himalaya, where the compiled data comes from, the magnitude of glacial advance and retreat were very modest (94). Moreover, the viscoelastic response to glacial erosion may have a shorter relaxation time in this landscape because of lower middle crust viscosity (95). The proposed coupling between tectonics and erosion could further dampen the response of the landscape to long periods in climate forcing when compared to less active (colder) areas.

San Gabriel Mountains



Central Himalaya



Taiwan

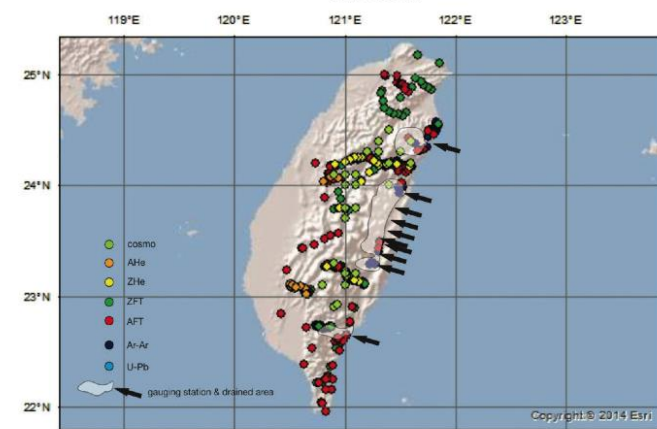


fig. S5. Location maps of data for fluvial landscapes. Maps showing the locations of the compiled data for the landscapes dominated by fluvial processes (Fig. 2B).

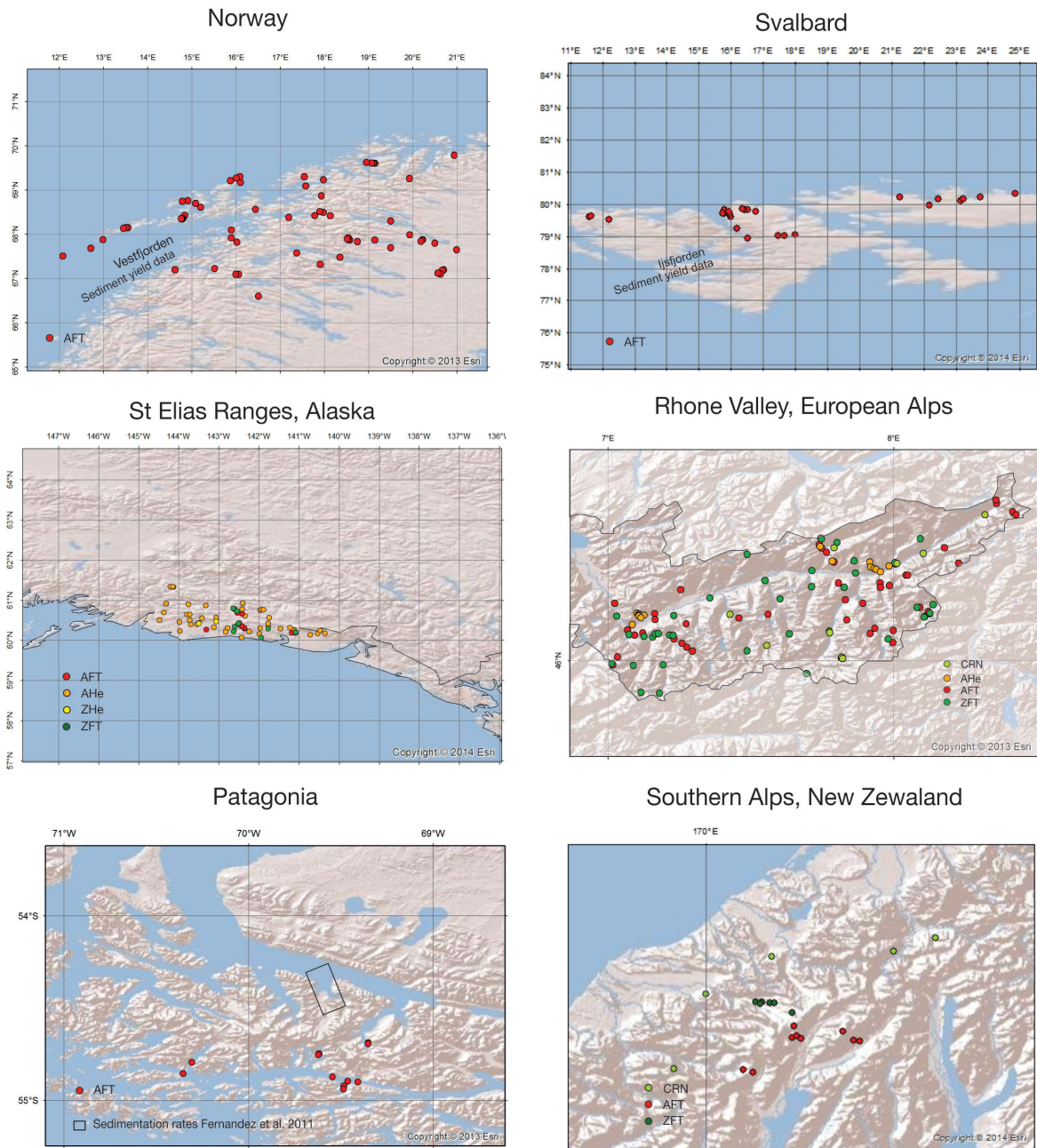


fig. S6. Location maps of data for glaciated landscapes. Maps showing the locations of the compiled data for the landscapes dominated by glacial processes (Fig. 2A). The estimated erosion rates for Pacific NW were directly compiled from *Koppes and Montgomery (56)*.

table S1. Landscape setting and fitted scaling exponents. Summary of the geologic settings of the landscapes considered in this study along with the scaling exponents of the best fitting power laws.

Landscape	Description of geologic setting*	Scaling exponent (α)	Standard Error (SE)
Southern Alps, New Zealand	Active collision between the Australian and Pacific Plates, glaciated	-0.19	0.02
St. Elias Range	Ongoing collision of the Yakutat Block in the North American Plate, glaciated	-0.24	0.06
Rhone valley, central European Alps	Continent-continent collision of the Adriatic Micro-plate into Eurasia, very slow convergence, glaciated	-0.11	0.08
Patagonia	Active subduction of the Antarctic Plate under the South American Plate, glaciated	-0.71	0.10
Svalbard	Tectonically inactive; passive margin, glaciated	-0.22	0.04
Pacific NW	Active subduction of the Juan de Fuca Plate underneath the North American Plate, glaciated	-0.25	0.1
Norway	Tectonically inactive; passive margin, glaciated	-0.48	0.12
Central Himalayas	Ongoing continent-continent collision of the Indian and Eurasian Plates	0.05	0.07
San Gabriel Mountains	Active convergence at a restraining bend of the San Andreas Fault	-0.03	0.20
Taiwan	Active collision between the Philippian Sea Plate and Eurasia	-0.02	0.04

*See references in table S2 for data compiled and details pertaining to each landscape.

table S2. Tabulated data used in this study. Data compilation from previously published studies, used to evaluate erosion rates across diverse time scales.

Longitude	Latitude	Age* (My)	Error* (My)	System	Erosion rate [mm/year]	Ref.
New Zealand						
170.079	-43.652	3.2	1.6	AFT	1.62	(96)
170.1	-43.657	7	1.8	AFT	0.66	(96)
170.184	-43.583	4.4	0.9	AFT	1.12	(96)
170.194	-43.58	3.2	0.7	AFT	1.62	(96)
170.203	-43.586	5.1	1.1	AFT	0.94	(96)
170.293	-43.571	10.2	3.3	AFT	0.41	(96)
170.315	-43.59	5.7	1.1	AFT	0.78	(96)
170.328	-43.591	6.1	1.4	AFT	0.72	(96)
170.115	-43.511	0.6	0.3	AFT	6.11	(96)
170.136	-43.51	1.5	0.5	AFT	2.44	(96)
170.146	-43.509	0.8	0.5	AFT	4.58	(96)
170.184	-43.531	3.8	1.3	AFT	1.24	(96)
170.187	-43.558	3.3	1.4	AFT	1.47	(96)
170.119	-43.507	1.5	0.3	ZFT	4.44	(96)
170.106	-43.507	0.9	0.1	ZFT	7.41	(96)
170.115	-43.511	1	0.1	ZFT	6.67	(96)
170.136	-43.51	1.8	0.2	ZFT	3.70	(96)
170.146	-43.509	1.3	0.2	ZFT	5.13	(96)
170.184	-43.531	4.9	0.5	ZFT	1.36	(96)
169.93	-43.65	211	25	CRN [year]	3.70	(97)
170	-43.49	606	73	CRN	1.38	(97)
170.14	-43.41	421	43	CRN	2.03	(97)
170.4	-43.4	103	22	CRN	7.78	(97)
170.49	-43.37	119	33	CRN	6.61	(97)
171.04	-43.08	86	13	CRN	8.96	(97)
Norway						
20.62	67.103	615.3	52	AFT	0.01	(98)
20.183	67.842	251.5	29.8	AFT	0.02	(98)
19.14	67.869	211	21	AFT	0.02	(98)
18.511	67.897	254.3	20.9	AFT	0.01	(98)
18.128	68.421	140.3	8.3	AFT	0.01	(98)
17.98	68.493	126.5	7.8	AFT	0.01	(98)
17.929	68.87	143	12.6	AFT	0.01	(98)
17.907	67.326	268.6	32.3	AFT	0.01	(98)
17.539	69.306	163.8	13.2	AFT	0.01	(98)
17.369	67.576	209.2	16.1	AFT	0.01	(98)
17.194	68.385	124.6	6.3	AFT	0.02	(98)
16.096	69.175	144.9	11.1	AFT	0.02	(98)

Longitude	Latitude	Age* (My)	Error* (My)	System	Erosion rate [mm/year]	Ref.
16.093	69.175	166	20.6	AFT	0.02	(98)
15.992	67.095	157.4	11	AFT	0.02	(98)
15.89	68.099	110.8	6.9	AFT	0.02	(98)
15.872	69.214	127.3	11.1	AFT	0.02	(98)
15.197	68.611	176.6	13.4	AFT	0.02	(98)
15.08	68.701	195.6	23	AFT	0.02	(98)
14.911	68.759	247.1	18.9	AFT	0.02	(98)
14.79	68.355	173.1	13.4	AFT	0.02	(98)
14.786	68.355	161.2	13.7	AFT	0.02	(98)
14.783	68.751	238.2	27.8	AFT	0.02	(98)
14.782	68.354	159	16.3	AFT	0.02	(98)
14.772	68.354	153.6	13.7	AFT	0.02	(98)
14.769	68.353	153.6	12	AFT	0.03	(98)
14.767	68.354	158.5	15.1	AFT	0.02	(98)
14.763	68.357	151.5	10.9	AFT	0.02	(98)
14.762	68.355	143.8	15.8	AFT	0.02	(98)
14.761	68.356	147.4	10.6	AFT	0.01	(98)
14.618	67.203	170.5	12.3	AFT	0.02	(98)
13.546	68.154	180.8	20.8	AFT	0.03	(98)
13.505	68.149	111.2	23.8	AFT	0.03	(98)
13.455	68.139	120.2	13.6	AFT	0.02	(98)
12.714	67.688	124.5	9.7	AFT	0.03	(98)
12.078	67.506	123.6	9.4	AFT	0.01	(98)
20.935	69.791	214.3	24.2	AFT	0.03	(99)
20.667	67.183	263.8	24.6	AFT	0.03	(99)
20.569	67.127	317.7	28.9	AFT	0.02	(99)
20.226	67.877	303.5	35.9	AFT	0.02	(99)
20.209	67.869	267.9	29.3	AFT	0.02	(99)
20.183	67.842	225.1	22.5	AFT	0.03	(99)
20.183	67.842	212.4	23.5	AFT	0.01	(99)
19.929	67.991	242.7	22.7	AFT	0.02	(99)
19.924	69.264	170.4	14.9	AFT	0.03	(99)
19.146	69.606	229.9	25.5	AFT	0.02	(99)
19.109	69.609	241.4	26.1	AFT	0.03	(99)
19.105	69.601	189	18.6	AFT	0.03	(99)
19.066	69.608	202.6	19.7	AFT	0.04	(99)
18.951	69.626	216.2	22.1	AFT	0.03	(99)
18.745	67.836	112.8	13.8	AFT	0.02	(99)
18.565	67.872	157.3	20.9	AFT	0.03	(99)
18.544	67.926	220.4	24.8	AFT	0.04	(99)
18.538	67.877	204.6	23.6	AFT	0.03	(99)
18.35	67.483	243	23.9	AFT	0.03	(99)

Longitude	Latitude	Age* (My)	Error* (My)	System	Erosion rate [mm/year]	Ref.
17.978	69.236	173	17.1	AFT	0.02	(99)
17.888	68.516	134	16.1	AFT	0.02	(99)
17.778	68.417	124.3	12.3	AFT	0.01	(99)
17.575	69.089	167.7	20.6	AFT	0.02	(99)
16.437	68.56	179.7	20.9	AFT	0.02	(99)
16.08	69.306	128.2	13.7	AFT	0.02	(99)
16.055	67.097	113.5	11.7	AFT	0.02	(99)
16.023	67.826	89.9	8.3	AFT	0.02	(99)
16.01	69.277	141.8	14.4	AFT	0.02	(99)
15.889	67.921	89.4	9.6	AFT	0.02	(99)
15.512	67.229	143.6	16.7	AFT	0.02	(99)
14.839	68.423	149.2	15.1	AFT	0.02	(99)
12.987	67.877	129.4	15.2	AFT	0.03	(99)
20.995	67.649	322.4	36.1	AFT	0.02	(99)
16.509	66.605	283	20	AFT	0.02	(100)
20.7	67.2	158	32	AFT	0.02	(101)
20.5	67.8	411	65	AFT	0.03	(101)
19.5	68.3	195	35	AFT	0.03	(101)
19.5	68.3	221	39	AFT	0.03	(101)
19.5	67.7	181	31	AFT	0.03	(101)
19.5	67.7	225	37	AFT	0.03	(101)
Svalbard						
11.595	79.593	78	6	AFT	0.05	(102)
11.659	79.632	92	7	AFT	0.04	(102)
15.803	79.709	171	84	AFT	0.02	(102)
15.809	79.824	137	17	AFT	0.03	(102)
15.736	79.719	76	18	AFT	0.05	(102)
16.769	79.763	97	35	AFT	0.04	(102)
15.999	79.611	175	30	AFT	0.02	(102)
17.46	79.013	62	5	AFT	0.06	(102)
17.67	79.025	64	5	AFT	0.06	(102)
17.989	79.034	84	5	AFT	0.04	(102)
12.206	79.521	108	5	AFT	0.03	(102)
15.972	79.699	109	9	AFT	0.03	(102)
15.972	79.699	131	10	AFT	0.03	(102)
16.441	79.839	116	6	AFT	0.03	(102)
16.441	79.839	130	8	AFT	0.03	(102)
16.513	79.84	75	9	AFT	0.05	(102)
16.418	79.826	137	16	AFT	0.03	(102)
16.368	79.842	138	11	AFT	0.03	(102)
15.931	79.783	121	11	AFT	0.03	(102)

Longitude	Latitude	Age* (My)	Error* (My)	System	Erosion rate [mm/year]	Ref.
16.531	78.928	80	9	AFT	0.05	(102)
16.194	79.246	82	6	AFT	0.04	(102)
23.135	80.108	133	5	AFT	0.03	(102)
22.459	80.166	130	5	AFT	0.03	(102)
22.182	79.979	173	8	AFT	0.02	(102)
23.238	80.169	126	33	AFT	0.03	(102)
21.265	80.217	128	9	AFT	0.03	(102)
23.764	80.228	114	17	AFT	0.03	(102)
24.847	80.336	214	10	AFT	0.02	(102)
Rhône						
7.458051	46.14778	13.1	1.6	AFT	0.28	(103)
7.695287	45.95454	12.7	1	AFT	0.29	(103)
7.695287	45.95454	14.8	1.3	AFT	0.25	(103)
7.695287	45.95454	33.5	1.9	ZFT	0.20	(103)
7.695287	45.95454	33.3	2.4	ZFT	0.20	(103)
7.800845	46.41212	8.9	0.8	ZFT	0.75	(104)
7.738836	46.40403	6.7	0.9	AFT	0.55	(105)
7.741793	46.39782	8.1	0.7	AFT	0.45	(105)
7.747095	46.39258	7	0.8	AFT	0.52	(105)
7.764565	46.37868	7	1	AFT	0.52	(105)
7.784384	46.34713	7.5	0.5	AFT	0.49	(105)
7.790083	46.34451	5.9	0.6	AFT	0.62	(105)
7.741793	46.39782	4.4	2	AHe	0.45	(105)
7.784384	46.34713	5.4	1.8	AHe	0.37	(105)
7.074164	46.09088	11.4	1	ZFT	0.58	(106)
7.11621	45.88933	17	1.6	ZFT	0.39	(106)
7.126825	46.08393	11.2	1.3	ZFT	0.60	(106)
7.156702	46.08122	13.5	0.9	ZFT	0.49	(106)
7.165562	46.09321	13.4	1.5	ZFT	0.50	(106)
7.17603	46.09422	16.3	1.8	ZFT	0.41	(106)
7.215615	46.08954	17.7	2.3	ZFT	0.38	(106)
7.227902	46.0883	19.7	1.6	ZFT	0.34	(106)
7.230226	46.15694	25.9	2.6	ZFT	0.26	(106)
7.356604	46.21855	22.9	1.6	ZFT	0.29	(106)
7.074164	46.09088	5.7	0.4	AFT	0.64	(106)
7.093571	46.08869	3.2	0.4	AFT	1.15	(106)
7.122096	46.09696	1.8	0.15	AFT	2.04	(106)
7.126825	46.08393	1.4	0.15	AFT	2.62	(106)
7.164431	46.16382	3.1	0.2	AFT	1.18	(106)
7.227902	46.0883	6.1	0.7	AFT	0.60	(106)
7.258895	46.05966	11.3	2.1	AFT	0.32	(106)

Longitude	Latitude	Age* (My)	Error* (My)	System	Erosion rate [mm/year]	Ref.
7.276508	46.04647	10.8	4	AFT	0.34	(106)
7.295145	46.03345	13.3	6	AFT	0.28	(106)
7.011996	45.98874	15.7	1.6	ZFT	0.42	(107)
7.030244	46.15469	17.2	1.7	ZFT	0.39	(107)
7.088627	45.98258	12.2	1.2	ZFT	0.55	(107)
7.486721	46.37064	216	27	ZFT	0.03	(107)
7.549175	46.27942	25.6	2.9	ZFT	0.26	(107)
7.601914	46.21459	23.6	3	ZFT	0.28	(107)
7.634266	46.09382	35.6	2.9	ZFT	0.19	(107)
7.71228	46.2581	22.3	2.3	ZFT	0.30	(107)
7.71321	46.31387	9.1	0.9	ZFT	0.73	(107)
7.746943	46.42465	117	12	ZFT	0.06	(107)
7.774872	46.1032	27.5	2.5	ZFT	0.24	(107)
7.82574	46.25552	19.8	1.9	ZFT	0.34	(107)
7.860434	46.34805	7.9	0.8	ZFT	0.84	(107)
7.866206	46.30557	8	0.8	ZFT	0.83	(107)
7.980214	46.07497	17.5	1.5	ZFT	0.38	(107)
8.003653	46.34158	10.1	0.9	ZFT	0.66	(107)
8.080791	46.18617	10.1	1	ZFT	0.66	(107)
8.09313	46.42638	11.7	1.1	ZFT	0.57	(107)
8.105879	46.15121	16.8	1.5	ZFT	0.40	(107)
8.105879	46.15121	14.9	1.2	ZFT	0.45	(107)
8.125577	46.16332	17.7	1.9	ZFT	0.38	(107)
8.126125	46.16575	11.6	1	ZFT	0.57	(107)
8.137647	46.196	9.4	1	ZFT	0.71	(107)
7.011996	45.98874	9.3	2	AFT	0.39	(107)
7.016673	45.98471	6.7	1.2	AFT	0.55	(107)
7.022908	46.20009	3.7	0.4	AFT	0.99	(107)
7.030244	46.15469	3.5	0.4	AFT	1.05	(107)
7.034207	46.01302	5.6	0.9	AFT	0.65	(107)
7.068751	46.10742	3.9	0.6	AFT	0.94	(107)
7.088627	45.98258	4.8	0.7	AFT	0.76	(107)
7.164923	46.14322	2.4	0.3	AFT	1.53	(107)
7.230797	46.07509	6.6	0.8	AFT	0.56	(107)
7.254517	46.24703	5.3	1	AFT	0.69	(107)
7.274454	46.1282	10.1	1.5	AFT	0.36	(107)
7.486721	46.37064	5.6	0.7	AFT	0.65	(107)
7.549175	46.27942	13.4	1.5	AFT	0.27	(107)
7.560199	46.16166	9.8	2.3	AFT	0.37	(107)
7.601914	46.21459	11.7	2.6	AFT	0.31	(107)
7.634266	46.09382	10.6	1.2	AFT	0.35	(107)
7.71228	46.2581	10.8	1.3	AFT	0.34	(107)

Longitude	Latitude	Age* (My)	Error* (My)	System	Erosion rate [mm/year]	Ref.
7.82574	46.25552	7.2	1.1	AFT	0.51	(107)
8.125577	46.16332	5.2	0.7	AFT	0.71	(107)
8.126125	46.16575	3.6	0.6	AFT	1.02	(107)
8.137647	46.196	2.4	0.6	AFT	1.53	(107)
7.774872	46.1032	9.5	1.5	AFT	0.39	(107)
8.107853	46.15389	11.1	3.5	AFT	0.33	(107)
7.71321	46.31387	3.8	0.4	AFT	0.96	(104, 107)
7.744232	46.42848	5.5	0.7	AFT	0.67	(104, 107)
7.746943	46.42465	6.8	0.8	AFT	0.54	(104, 107)
7.860434	46.34805	3.6	0.6	AFT	1.02	(104, 107)
7.866206	46.30557	1.7	0.2	AFT	2.16	(104, 107)
8.09313	46.42638	5.6	0.6	AFT	0.65	(104, 107)
8.091414	46.18638	2.9	0.6	AFT	1.26	(107–109)
8.120622	46.17091	3.4	0.9	AFT	1.08	(107–109)
7.917	46.344	4.6	0.2	AHe	0.43	(110)
7.919	46.327	4.3	0.5	AHe	0.47	(110)
7.931	46.322	3	0.6	AHe	0.67	(110)
7.938	46.318	2.9	0.4	AHe	0.69	(110)
7.983	46.33	3.1	0.6	AHe	0.65	(110)
7.953	46.31	1.6	0.5	AHe	1.25	(110)
7.102	46.165	6.7	1.1	AHe	0.30	(110)
7.108	46.162	7.5	0.6	AHe	0.27	(110)
7.107	46.158	5.3	0.3	AHe	0.38	(110)
7.108	46.156	6.4	1	AHe	0.31	(110)
7.127	46.158	4.9	1	AHe	0.41	(110)
7.116	46.149	4.6	0.4	AHe	0.43	(110)
7.086	46.126	4.4	0.5	AHe	0.45	(110)
7.179977	45.88601	31.5		ZFT	0.21	Vance, published in (2)
7.192981	45.985	29.5		ZFT	0.23	Vance, published in (2)
7.486994	46.034	35.9		ZFT	0.19	Vance, published in (2)
8.357095	46.5608	7.1	0.9	AFT	0.52	(111)
7.829966	46.21187	4.9	0.49	AFT	0.75	(108, 109)
7.835936	46.14213	10.4	1.04	AFT	0.35	(108, 109)
7.917697	46.09459	6.4	0.64	AFT	0.57	(108, 109)
7.74031	46.40151	4.6	0.46	AFT	0.80	(108, 109)
7.800845	46.41212	3.5	0.35	AFT	1.05	(108, 109)
7.892069	46.2004	4.6	0.46	AFT	0.80	(108, 109)
7.917697	46.09459	6.3	0.63	AFT	0.58	(108, 109)
7.934022	46.11251	5.5	0.55	AFT	0.67	(108, 109)

Longitude	Latitude	Age* (My)	Error* (My)	System	Erosion rate [mm/year]	Ref.
7.996238	46.06185	6.4	0.64	AFT	0.57	(108, 109)
7.998618	46.10501	7	0.7	AFT	0.52	(108, 109)
8.41536	46.51915	7.1	0.71	AFT	0.52	(108, 109)
8.426243	46.50849	6.3	0.63	AFT	0.58	(108, 109)
7.980214	46.07497	5.6	0.56	AFT	0.65	(107–109)
8.080791	46.18617	2.6	0.26	AFT	1.41	(107)
8.105879	46.15121	6.2	0.62	AFT	0.59	(107)
7.807043	46.27132	5.6	0.56	AFT	0.65	(109)
7.951678	46.27076	3.4	0.34	AFT	1.08	(109)
7.953479	46.25546	3.5	0.35	AFT	1.05	(109)
7.984674	46.26251	6.7	0.67	AFT	0.55	(109)
8.005834	46.33651	3	0.3	AFT	1.22	(109)
8.042652	46.29766	4.4	0.44	AFT	0.83	(109)
8.049401	46.29771	4.2	0.42	AFT	0.87	(109)
8.177114	46.39343	4.5	0.45	AFT	0.81	(109)
8.226788	46.34024	7.2	0.72	AFT	0.51	(109)
8.360407	46.54849	4.8	0.48	AFT	0.76	(109)
8.003653	46.34158	3.4	0.34	AFT	1.08	(104, 107, 109)
7.426636	46.16071	110	--	CRN [year]	0.37	(42)
7.555878	46.05269	110	--	CRN	6.44	(42)
7.555878	46.05269	240	--	CRN	2.89	(42)
7.555878	46.05269	260	--	CRN	2.68	(42)
7.555878	46.05269	390	--	CRN	1.76	(42)
7.775821	46.09723	610	--	CRN	1.13	(42)
7.790663	46.39408	580	--	CRN	1.28	(42)
7.816601	46.00983	390	--	CRN	1.87	(42)
7.817905	46.01163	1320	--	CRN	0.52	(42)
7.820456	46.00712	360	--	CRN	1.87	(42)
8.011139	46.3392	150	--	CRN	4.65	(42)
8.102503	46.37469	550	--	CRN	1.32	(42)
8.319154	46.50853	1080	--	CRN	0.69	(42)
Patagonia						
-69.3511	-54.6874	27.2	5.8	AFT	0.13	(63)
-69.3508	-54.6926	18.5	3.3	AFT	0.20	(63)
-69.6178	-54.746	21.9	2.7	AFT	0.17	(63)
-69.6203	-54.7527	28.8	4.7	AFT	0.13	(63)
-70.3071	-54.7931	17.3	2.2	AFT	0.22	(63)
-70.3544	-54.8551	9.1	2.7	AFT	0.44	(63)
-69.5452	-54.8735	30.8	4.1	AFT	0.12	(63)
-69.4631	-54.8962	35.9	3.9	AFT	0.11	(63)
-69.4072	-54.9006	29.4	4.4	AFT	0.12	(63)

Longitude	Latitude	Age* (My)	Error* (My)	System	Erosion rate [mm/year]	Ref.
-73.2935	-53.1567	18.2	3.1	AFT	0.27	(63)
-73.1035	-53.345	18.3	3.1	AFT	0.27	(63)
-72.9127	-53.4297	19.8	3.1	AFT	0.25	(63)
-72.3527	-53.5327	18.6	3.3	AFT	0.26	(63)
-72.4032	-53.57	19	3.5	AFT	0.26	(63)
-72.4032	-53.57	7.66	0.43	AHe	0.27	(63)
-72.4032	-53.57	10.69	1.83	AHe	0.18	(63)
-72.4032	-53.57	9.75	1.16	AHe	0.20	(63)
-72.3527	-53.5327	6.29	0.73	AHe	0.34	(63)
-72.3527	-53.5327	8.17	1.28	AHe	0.25	(63)
-72.3527	-53.5327	10.61	1.18	AHe	0.19	(63)
-72.5588	-53.5093	12.14	0.58	AHe	0.16	(63)
-72.5588	-53.5093	14.52	0.77	AHe	0.13	(63)
-72.9127	-53.4297	11.17	0.62	AHe	0.18	(63)
-72.9127	-53.4297	15.3	3.08	AHe	0.12	(63)
-72.5938	-53.4205	11.94	0.65	AHe	0.16	(63)
-73.1035	-53.345	7.71	0.57	AHe	0.27	(63)
-73.1035	-53.345	12.65	0.42	AHe	0.15	(63)
-73.2935	-53.1567	10.09	0.25	AHe	0.20	(63)
Central Himalayas						
87.151	26.848	0.6	-	CRN [ky]	1.00	(112)
87.151	26.848	1.2	-	CRN	0.50	(112)
87.151	26.848	0.7	-	CRN	0.90	(112)
86.725	25.543	0.75	-	CRN	0.80	(112)
87.32795	28.32557	9.3	1.6	(U-Th)/He	0.64	(113)
87.34344	28.16075	5.2	0.9	(U-Th)/He	1.15	(113)
87.3779	28.07256	2.4	0.2	(U-Th)/He	2.55	(113)
87.36294	27.71859	1.9	0.4	(U-Th)/He	3.10	(113)
87.36326	27.68617	1.9	0.3	(U-Th)/He	3.08	(113)
87.34866	27.64063	3	0	(U-Th)/He	1.98	(113)
87.32592	27.61013	5.4	0.8	(U-Th)/He	1.11	(113)
87.27118	27.5627	5.2	0.7	(U-Th)/He	1.16	(113)
87.16963	27.48586	6.3	0.9	(U-Th)/He	0.95	(113)
87.13879	27.44907	3.7	0.7	(U-Th)/He	1.63	(113)
87.17398	27.37131	4.6	0.7	(U-Th)/He	1.30	(113)
87.19312	27.35009	5.3	1.7	(U-Th)/He	1.14	(113)
87.25274	27.09443	9.7	1.4	(U-Th)/He	0.62	(113)
87.31367	26.93132	8.6	0.7	(U-Th)/He	0.70	(113)
87.3234	27.70102	1.9	0.3	(U-Th)/He	3.08	(113)
87.19837	27.72844	2.5	0.4	(U-Th)/He	2.40	(113)
87.15656	27.78867	4.1	0.7	(U-Th)/He	1.45	(113)

Longitude	Latitude	Age* (My)	Error* (My)	System	Erosion rate [mm/year]	Ref.
87.08285	27.83099	4.2	0.6	(U-Th)/He	1.43	(113)
86.84572	28.16815	10.5	1.3	(U-Th)/He	0.57	(113)
87.19891	27.44656	14.9	2.9	Ar/Ar	0.74	(113)
87.24045	27.48158	9.6	0.5	Ar/Ar	1.15	(113)
87.27085	27.52159	10.2	0.5	Ar/Ar	1.08	(113)
87.27118	27.5627	12.8	3.5	Ar/Ar	0.86	(113)
87.27327	27.56478	16.9	5.1	Ar/Ar	0.65	(113)
87.2723	27.56471	15.7	3.7	Ar/Ar	0.70	(113)
87.2676	27.59143	14.9	1.4	Ar/Ar	0.74	(113)
87.26477	27.61003	8.5	0.3	Ar/Ar	1.29	(113)
87.23507	27.62432	8.2	0.2	Ar/Ar	1.34	(113)
87.22486	27.63135	8.3	1.3	Ar/Ar	1.32	(113)
87.2136	27.64352	7.9	0.8	Ar/Ar	1.40	(113)
87.36294	27.71859	5.8	0.4	Ar/Ar	1.90	(113)
87.36176	27.69293	9.2	0.9	Ar/Ar	1.19	(113)
87.36326	27.68617	7.8	0.5	Ar/Ar	1.41	(113)
87.34866	27.64063	8.4	0.8	Ar/Ar	1.31	(113)
87.32592	27.61013	8.4	0.5	Ar/Ar	1.31	(113)
87.21541	27.52523	19.7	6.3	Ar/Ar	0.56	(113)
87.16963	27.48586	16.4	2.4	Ar/Ar	0.67	(113)
87.13879	27.44907	15.7	3	Ar/Ar	0.70	(113)
87.14009	27.39522	15.3	4.4	Ar/Ar	0.72	(113)
87.19312	27.35009	66	39.8	Ar/Ar	0.17	(113)
Taiwan						
121.1501	24.0493	2.06	0.19	ZHe	3.16	(114)
121.1544	24.2503	1.46	0.1	ZHe	4.45	(114)
121.3065	24.1805	0.85	0.21	ZHe	7.65	(114)
121.2238	24.1156	23.27	-	ZHe	0.28	(114)
121.2921	24.2005	3.68	1.89	ZHe	1.77	(114)
121.1459	24.0335	11.42	-	ZHe	0.57	(114)
121.2593	24.2235	31.5	-	ZHe	0.21	(114)
121.1229	24.2514	1.49	0.14	ZHe	4.36	(114)
121.0909	24.2515	1.51	0.02	ZHe	4.30	(114)
121.05	24.2305	2.02	0.11	ZHe	3.22	(114)
121.0063	24.2117	1.98	0.06	ZHe	3.28	(114)
120.9108	24.1886	22.7	-	ZHe	0.29	(114)
121.3729	24.1906	1.12	0.23	ZHe	5.80	(114)
121.4753	24.1924	0.49	0.03	ZHe	13.27	(114)
121.584	24.1772	1.02	0.11	ZHe	6.37	(114)
121.587	24.1694	1.11	0.14	ZHe	5.86	(114)
121.1324	23.1351	0.57	0.04	ZHe	11.40	(114)

Longitude	Latitude	Age* (My)	Error* (My)	System	Erosion rate [mm/year]	Ref.
121.0824	23.1414	0.46	0.02	ZHe	14.13	(114)
121.0114	23.1845	0.57	0.08	ZHe	11.40	(114)
121.0153	23.2129	0.7	0.05	ZHe	9.29	(114)
121.0006	23.2274	0.76	0.08	ZHe	8.55	(114)
120.8427	23.2623	24.07	-	ZHe	0.27	(114)
120.9516	23.7959	2.93	0.43	ZHe	2.22	(114)
121.4	24.5	381	190	CRN [year]	2.00	(115)
121.2	24.3	414	96	CRN	1.80	(115)
121.3	24.4	558	187	CRN	1.40	(115)
121.3	24.4	156	43	CRN	4.90	(115)
121.3	24.3	601	193	CRN	1.30	(115)
121.3	24.3	126	32	CRN	6.10	(115)
121	24.1	1029	224	CRN	0.70	(115)
120.9	24.1	832	177	CRN	0.90	(115)
121.1	24.1	745	188	CRN	1.00	(115)
121	24	3378	566	CRN	0.20	(115)
121.1	24.1	417	100	CRN	1.80	(115)
121.1	24	1006	296	CRN	0.80	(115)
121	23.7	336	80	CRN	2.30	(115)
121	23.8	435	93	CRN	1.80	(115)
121.1	23.8	203	58	CRN	3.80	(115)
121.1	23.8	76	25	CRN	10.00	(115)
121.1	23.8	621	115	CRN	1.20	(115)
120.9	23.3	270	77	CRN	2.80	(115)
120.8	23.1	330	83	CRN	2.30	(115)
121.6	24.4	224	94	CRN	3.40	(115)
121.5	24.3	121	44	CRN	6.30	(115)
121.4	24.2	173	49	CRN	4.40	(115)
121.4	24.2	738	234	CRN	1.00	(115)
121.6	24.2	410	119	CRN	1.90	(115)
121.4	24	231	79	CRN	3.30	(115)
121.4	24	158	53	CRN	4.80	(115)
121.4	24	118	35	CRN	6.50	(115)
121.1	23.2	306	77	CRN	2.50	(115)
121	23.2	144	42	CRN	5.30	(115)
121	23.2	87	40	CRN	8.80	(115)
121	23.2	108	42	CRN	7.00	(115)
121	23.2	140	44	CRN	5.40	(115)
121	23.1	186	56	CRN	4.10	(115)
120.9	22.9	322	69	CRN	2.40	(115)
120.9	22.9	246	72	CRN	3.10	(115)
120.93	22.92	230	60	CRN	3.30	(115)

Longitude	Latitude	Age* (My)	Error* (My)	System	Erosion rate [mm/year]	Ref.
120.621	23.073	5.59	0.61	AFT	0.63	(116)
120.65	23.034	3.37	0.64	AFT	1.04	(116)
120.662	23.048	2.6	1.1	AFT	1.35	(116)
121.017	22.65	0.7	0.3	AFT	5.00	(116)
121.042	22.767	0.4	0.1	AFT	8.75	(116)
121.067	22.9	0.7	0.2	AFT	5.00	(116)
121.3	23.432	0.6	0.2	AFT	5.83	(116)
121.01	22.648	0.918	0.35	AFT	3.81	(116)
120.98	22.592	1.41	1	AFT	2.48	(116)
120.952	22.511	1.17	0.37	AFT	2.99	(116)
120.891	22.377	2.26	0.66	AFT	1.55	(116)
120.886	22.249	2.35	0.43	AFT	1.49	(116)
120.908	22.589	0.388	0.17	AFT	9.02	(116)
120.932	22.623	0.754	0.25	AFT	4.64	(116)
120.931	22.616	0.558	0.21	AFT	6.27	(116)
120.934	22.613	0.584	0.293	AFT	5.99	(116)
120.943	22.62	0.608	0.22	AFT	5.76	(116)
120.841	22.269	1.6	0.34	AFT	2.19	(116)
120.762	22.216	1.83	0.56	AFT	1.91	(116)
120.831	21.957	27.9	2	AFT	0.13	(116)
120.883	22.155	2.26	0.38	AFT	1.55	(116)
120.787	22.041	3.95	1.42	AFT	0.89	(116)
120.792	22.034	5.49	1.2	AFT	0.64	(116)
120.824	22.161	1.69	0.36	AFT	2.07	(116)
120.632	22.389	3.11	0.64	AFT	1.13	(116)
120.7	22.529	2.37	0.64	AFT	1.48	(116)
120.648	22.713	3.58	0.66	AFT	0.98	(116)
120.52	23.082	31.9	2.4	AFT	0.11	(116)
120.544	23.071	22.8	1.3	AFT	0.15	(116)
120.621	23.073	5.59	0.61	AFT	0.63	(116)
120.659	23.031	3.37	0.64	AFT	1.04	(116)
120.67	23.046	2.62	1.08	AFT	1.34	(116)
120.61	23.438	33.6	2.3	AFT	0.10	(116)
120.617	23.432	29.3	2	AFT	0.12	(116)
120.728	23.465	32.4	2	AFT	0.11	(116)
120.821	23.512	28.2	8.6	AFT	0.12	(116)
120.841	23.284	2.01	0.64	AFT	1.74	(116)
120.942	23.263	1.5	1.06	AFT	2.33	(116)
120.91	24.175	0.939	0.357	AFT	3.73	(116)
120.874	24.171	7.82	0.83	AFT	0.45	(116)
120.817	23.892	11.4	1.2	AFT	0.31	(116)
120.73	24.197	28.5	1.6	AFT	0.12	(116)

Longitude	Latitude	Age* (My)	Error* (My)	System	Erosion rate [mm/year]	Ref.
120.939	23.793	2.47	0.43	AFT	1.42	(116)
120.938	23.566	73	11	AFT	0.05	(116)
120.865	23.546	1.52	0.51	AFT	2.30	(116)
121.303	24.194	1.16	0.58	AFT	3.02	(116)
121.265	24.235	4.64	0.91	AFT	0.75	(116)
121.265	24.235	0.35	0.25	AFT	10.00	(116)
121.231	24.247	1.62	0.67	AFT	2.16	(116)
121.236	24.247	5.28	1.44	AFT	0.66	(116)
121.515	24.025	0.859	0.14	AFT	4.07	(116)
121.7597	24.4964	37	3.6	Rb-Sr and K-Ar	0.32	(117)
121.7597	24.4964	35	4.8	Rb-Sr and K-Ar	0.33	(117)
121.7597	24.4964	37.4	5.9	Rb-Sr and K-Ar	0.31	(117)
121.7594	24.4964	39.7	0.1	Rb-Sr and K-Ar	0.29	(117)
121.7594	24.4964	37	3	Rb-Sr and K-Ar	0.32	(117)
121.7576	24.5025	40.1	2	Rb-Sr and K-Ar	0.29	(117)
121.5772	24.1777	6.4	0.3	Rb-Sr and K-Ar	1.82	(117)
121.576	24.1803	3.5	0.5	Rb-Sr and K-Ar	3.33	(117)
121.5675	24.173	2.5	0.1	Rb-Sr and K-Ar	4.67	(117)
121.576	24.1803	4.2	-	Rb-Sr and K-Ar	2.78	(117)
121.7597	24.4964	33.1	-	Rb-Sr and K-Ar	0.35	(117)
121.7576	24.5025	38	-	Rb-Sr and K-Ar	0.31	(117)
121.8226	24.4922	88.2	-	Rb-Sr and K-Ar	0.13	(117)
120.7613	22.7285	23	1.2	ZFT	0.34	(118)
120.8538	22.7123	5.3	0.7	ZFT	1.48	(118)
120.8582	22.7259	3.6	0.4	ZFT	2.18	(118)
120.8765	22.7266	5.2	0.8	ZFT	1.51	(118)
120.9177	22.5278	5.4	0.6	ZFT	1.45	(118)
120.9419	22.5966	3.5	0.3	ZFT	2.24	(118)
120.9617	22.6	4.2	0.5	ZFT	1.87	(118)
120.983	22.6088	4.7	0.4	ZFT	1.67	(118)
121.7519	24.4904	0.85	0.1	ZFT	9.22	(119)
121.6806	24.3203	1.31	0.14	ZFT	5.98	(119)
121.7994	24.4637	0.45	0.04	AFT	7.78	(119)
121.7519	24.4904	0.25	0.06	AFT	14.00	(119)
121.7075	24.322	0.29	0.03	AFT	12.07	(119)
121.5757	24.4344	0.37	0.05	AFT	9.46	(119)

Longitude	Latitude	Age* (My)	Error* (My)	System	Erosion rate [mm/year]	Ref.
121.6806	24.3203	0.47	0.05	AFT	7.45	(119)
121.662	24.3166	0.48	0.06	AFT	7.29	(119)
121.5331	24.1447	0.53	0.05	AFT	6.60	(119)
121.5084	24.1542	0.51	0.06	AFT	6.86	(119)
121.5518	24.1598	0.58	0.07	AFT	6.03	(119)
121.587	24.1919	0.37	0.05	AFT	9.46	(119)
121.5663	24.1768	0.54	0.05	AFT	6.48	(119)
121.5516	24.1219	0.47	0.04	AFT	7.45	(119)
121.5785	24.1351	0.47	0.05	AFT	7.45	(119)
121.4856	24.1278	0.4	0.03	AFT	8.75	(119)
121.4837	24.1581	0.28	0.02	AFT	12.50	(119)
121.3127	23.4826	0.42	0.15	AFT	8.33	(119)
121.6072	24.8842	3.1	8.3	ZFT	2.53	(119)
121.08	24.249	2.9	7	ZFT	2.70	(119)
120.9384	23.9404	2.6	8.7	ZFT	3.01	(119)
121.5741	24.1811	1.6	0.9 / 0.6	ZFT	4.90	(120)
121.47	24.2087	1	0.5 / 0.4	ZFT	7.83	(120)
121.3676	24.1715	1.9	0.9 / 0.6	ZFT	4.12	(120)
121.3248	24.1955	2.9	1.4 / 0.9	ZFT	2.70	(120)
121.2803	24.2399	26.1	13.9 / 9.1	ZFT	0.30	(120)
121.2245	24.2707	26.9	14.9 / 9.6	ZFT	0.29	(120)
121.1668	24.2555	3.1	1.5 / 1	ZFT	2.53	(120)
121.1277	24.2453	4.3	2.4 / 1.5	ZFT	1.82	(120)
121.0551	24.2248	2.9	1.4 / 1	ZFT	2.70	(120)
120.9695	24.1839	33.7	17.3 / 11.5	ZFT	0.23	(120)
120.8728	24.177	60.6	30.5 / 20.3	ZFT	0.13	(120)
120.9659	23.8801	4.7	2.4 / 1.6	ZFT	1.67	(120)
121.0335	23.7802	2.9	1.5 / 1	ZFT	2.70	(120)
121.0021	23.7895	3.3	1.7 / 1.1	ZFT	2.37	(120)
120.8994	23.7903	32.4	18.3 / 11.7	ZFT	0.24	(120)
121.1155	23.1275	1.5	0.9 / 0.6	ZFT	5.22	(120)
121.0657	23.1446	3	1.7 / 1.1	ZFT	2.61	(120)
121.0233	23.1838	2.1	1.2 / 0.8	ZFT	3.73	(120)
120.9605	23.2572	2	1.1 / 0.7	ZFT	3.92	(120)
120.8921	23.2896	57.9	22 / 14.1	ZFT	0.14	(120)
120.8441	23.2913	51.2	27.4 / 17.9	ZFT	0.15	(120)
120.6968	23.0607	67.7	34.5 / 22.9	ZFT	0.12	(120)
120.6212	23.0656	89.2	44.3 / 29.7	ZFT	0.09	(120)
121.8411	24.5592	1.2	+0.2 -0.2	ZFT	6.53	(120)
121.7834	24.8666	10.6	+2.8 -2.3	ZFT	0.74	(120)
121.7489	24.8855	23.5	+3.8 -3.3	ZFT	0.33	(120)
121.7129	24.91	29.1	+6.8 5.4	ZFT	0.27	(120)

Longitude	Latitude	Age* (My)	Error* (My)	System	Erosion rate [mm/year]	Ref.
121.691	24.9388	32.7	+4.9 4.3	ZFT	0.24	(120)
121.6376	24.9649	72.4	+13.5 -11.2	ZFT	0.11	(120)
121.8511	25.1059	211	+33.8 -29.1	ZFT	0.04	(120)
121.6545	25.1801	78.8	+18 -14.4	ZFT	0.10	(120)
121.5497	24.6625	3.7	+0.9 -0.7	ZFT	2.12	(120)
121.5213	24.6281	3.5	+1 -0.8	ZFT	2.24	(120)
121.4774	24.6512	4.6	+1.1 -0.9	ZFT	1.70	(120)
121.4382	24.6456	6.4	+1.1 -1	ZFT	1.22	(120)
121.3943	24.6716	14.2	+2.9 -2.5	ZFT	0.55	(120)
121.3567	24.7004	29.1	+6.8 -5.5	ZFT	0.27	(120)
121.3443	24.7578	53.8	+11.3 -9.2	ZFT	0.15	(120)
121.5062	24.7899	4.9	+0.9 -0.8	ZFT	1.60	(120)
121.3414	24.8539	38.6	+6.1 -5.3	ZFT	0.20	(120)
121.3272	24.8339	18.3	+1.1 -1.1	ZFT	0.43	(120)
120.952	22.5702	6	+1.3 -2.1	ZFT	1.31	(120)
120.8687	22.3606	44.4	+6.1 -5.4	ZFT	0.18	(120)
120.8457	22.2816	62.5	+18 -13.6	ZFT	0.13	(120)
120.801	22.2284	52.7	+9.9 -8.3	ZFT	0.15	(120)
120.7486	22.2198	100.1	+13.2 -11.8	ZFT	0.08	(120)
121.6027	24.167	66.8	0.3	Ar-Ar	0.27	(121)
121.7603	24.4908	73.3	0.5	Ar-Ar	0.25	(121)
121.762	24.5056	54.6	0.3	Ar-Ar	0.34	(121)
121.812	24.5369	69.9	0.8	Ar-Ar	0.26	(121)
121.5751	24.1785	7.7	0.1	Ar-Ar	1.65	(121)
121.5577	24.1831	11.4	0.2	Ar-Ar	1.11	(121)
121.5896	24.1909	8.2	0.1	Ar-Ar	1.54	(121)
121.6323	24.3774	12.7	0.1	Ar-Ar	1.00	(121)
121.7599	24.4908	20.1	0.2	Ar-Ar	0.63	(121)
121.762	24.5056	32.7	0.1	Ar-Ar	0.39	(121)
121.8134	24.4864	30.1	0.1	Ar-Ar	0.42	(121)
121.8201	24.5008	46.1	0.3	Ar-Ar	0.27	(121)
121.5896	24.1909	12	0.1	Ar-Ar	0.69	(121)
121.7603	24.4908	10.7	0.1	Ar-Ar	0.78	(121)
121.5577	24.1831	47.4	0.2	Ar-Ar	0.23	(121)
121.5577	24.1831	29	0.2	Ar-Ar	0.37	(121)
121.5896	24.1909	25.2	0.4	Ar-Ar	0.42	(121)
121.6323	24.3774	46.5	0.2	Ar-Ar	0.23	(121)
121.7603	24.4908	85.2	0.2	Ar-Ar	0.13	(121)
121.7603	24.4908	63.7	0.2	Ar-Ar	0.17	(121)
121.8134	24.4864	78.1	0.3	Ar-Ar	0.14	(121)
120.427	22.839	0.535	0.22	AFT	6.54	(122)

Longitude	Latitude	Age* (My)	Error* (My)	System	Erosion rate [mm/year]	Ref.
120.849	24.112	61.1	5.4	AFT	0.06	(122)
120.857	24.11	41.1	3.1	AFT	0.09	(122)
120.803	24.037	46.2	2.3	AFT	0.08	(122)
120.832	24.035	40.9	2.5	AFT	0.09	(122)
120.822	24.033	47.9	2.7	AFT	0.07	(122)
120.84	24.029	58.8	3.6	AFT	0.06	(122)
120.869	24.046	2.43	0.59	AFT	1.44	(122)
120.897	24.06	3.23	0.87	AFT	1.08	(122)
121.371	24.991	156	18	AFT	0.02	(122)
121.361	24.997	20.5	1.8	AFT	0.17	(122)
121.359	25	51.8	2.9	AFT	0.07	(122)
121.47	24.928	9.86	3.32	AFT	0.35	(122)
121.47	24.925	14.3	14.4	AFT	0.24	(122)
121.474	24.988	2.49	0.49	AFT	1.41	(122)
121.499	24.92	6.27	0.89	AFT	0.56	(122)
121.505	24.911	3.85	3.85	AFT	0.91	(122)
121.51	24.906	3.65	0.98	AFT	0.96	(122)
121.527	24.914	1.87	1.88	AFT	1.87	(122)
121.539	24.894	2.28	0.69	AFT	1.54	(122)
121.58	24.848	1.64	0.55	AFT	2.13	(122)
121.549	24.862	1.17	0.52	AFT	2.99	(122)
120.667	23.019	5.41	1.22	AFT	0.65	(122)
120.861	24.079	61	4.1	AFT	0.06	(122)
120.858	24.08	37.8	3.2	AFT	0.09	(122)
120.87	24.077	2.82	0.91	AFT	1.24	(122)
120.946	24.067	1.37	0.56	AFT	2.55	(122)
120.988	24.076	2.3	0.42	AFT	1.52	(122)
121.123	24.254	0.702	0.28	AFT	4.99	(122)
120.655	23.022	23.1	2.4	AFT	0.15	(122)
120.647	23.03	13.7	1.4	AFT	0.26	(122)
120.645	23.031	4.1	1.01	AFT	0.85	(122)
120.647	23.03	3.58	3.62	AFT	0.98	(122)
120.648	23.031	3.19	0.51	AFT	1.10	(122)
120.51	23.092	32.3	2	AFT	0.11	(122)
120.513	23.115	27.6	1.9	AFT	0.13	(122)
120.503	23.115	33	8	AFT	0.11	(122)
120.528	23.097	29.6	1.8	AFT	0.12	(122)
120.604	23.086	8.41	0.81	AFT	0.42	(122)
120.611	23.083	1.03	0.22	AFT	3.40	(122)
120.642	23.073	0.55	0.185	AFT	6.36	(122)
120.553	23.085	43.5	2.5	AFT	0.08	(122)
120.47	23.238	41.9	2.1	AFT	0.08	(122)

Longitude	Latitude	Age* (My)	Error* (My)	System	Erosion rate [mm/year]	Ref.
120.544	23.071	22.8	1.3	AFT	0.15	(122)
120.52	23.082	5.78	5.5	AHe	0.46	(122)
120.544	23.071	0.53	0.3	AHe	5.03	(122)
120.659	23.031	1.08	0.3	AHe	2.47	(122)
120.648	23.031	1.69	0.7	AHe	1.58	(122)
120.51	23.092	10.54	9.4	AHe	0.25	(122)
120.513	23.115	77.37	108.7	AHe	0.03	(122)
120.503	23.115	1.43	1.2	AHe	1.86	(122)
120.528	23.097	0.7	0.3	AHe	3.81	(122)
120.604	23.086	0.52	0.2	AHe	5.13	(122)
120.611	23.083	1	0.8	AHe	2.67	(122)
120.642	23.073	0.56	0.2	AHe	4.76	(122)
120.553	23.085	5.36	4.1	AHe	0.50	(122)
120.803	24.037	3.03	0.9	AHe	0.88	(122)
120.861	24.079	3.8	0.3	AHe	0.70	(122)
120.858	24.08	3.43	0.2	AHe	0.78	(122)
120.87	24.077	2.55	0.1	AHe	1.05	(122)
120.946	24.067	15.65	14.2	AHe	0.17	(122)
120.655	23.022	2.3	1.5	AHe	1.16	(122)
120.51	23.092	1.3	0.3	AHe	2.05	(122)
120.513	23.115	2.35	0.5	AHe	1.13	(122)
120.503	23.115	7.1	0.425	AHe	0.38	(122)
120.528	23.097	1.3	0.079	AHe	2.05	(122)
120.604	23.086	1.1	0.068	AHe	2.42	(122)
120.553	23.085	6.3	0.4	AHe	0.42	(122)
121.8203	24.5759	4.6	0.14	K-Ar white mica	1.92	(123)
121.8478	24.5419	1	0.18	K-Ar white mica	8.83	(123)
121.7502	24.4452	1.4	0.13	K-Ar white mica	6.31	(123)
121.7462	24.349	2.2	0.38	K-Ar white mica	4.02	(123)
120.7373	22.7408	50.8	1.14	K-Ar white mica	0.17	(123)
120.7449	22.7349	38	0.86	K-Ar white mica	0.23	(123)
120.7498	22.7327	30.8	0.69	K-Ar white mica	0.29	(123)
120.7611	22.7187	31.8	0.72	K-Ar white mica	0.28	(123)
120.7752	22.734	24.5	0.57	K-Ar white mica	0.36	(123)
120.7785	22.7294	10.1	0.23	K-Ar white mica	0.87	(123)
120.7781	22.7175	16.5	0.39	K-Ar white mica	0.54	(123)
120.7796	22.7128	11.3	0.27	K-Ar white	0.78	(123)

Longitude	Latitude	Age* (My)	Error* (My)	System	Erosion rate [mm/year]	Ref.
				mica		
120.8033	22.7194	3.1	0.24	K-Ar white mica	2.85	(123)
120.8014	22.7118	5.9	0.22	K-Ar white mica	1.50	(123)
120.8025	22.7056	5.8	0.24	K-Ar white mica	1.52	(123)
120.81	22.7086	5.2	0.38	K-Ar white mica	1.70	(123)
120.8218	22.7056	4.8	0.14	K-Ar white mica	1.84	(123)
120.8335	22.7173	7	0.34	K-Ar white mica	1.26	(123)
120.8407	22.7172	4.1	0.2	K-Ar white mica	2.15	(123)
120.8533	22.7175	4.92	0.26	K-Ar white mica	1.80	(123)
120.8672	22.7197	5.35	0.15	K-Ar white mica	1.65	(123)
121.5252	23.9783	3.97	0.23	K-Ar white mica	2.23	(123)
121.4798	23.9844	2.96	0.16	K-Ar white mica	2.98	(123)
121.4905	23.9367	4.32	0.14	K-Ar white mica	2.04	(123)
121.3164	23.499	8.15	0.23	K-Ar white mica	1.08	(123)
121.3033	23.4315	8.08	0.2	K-Ar white mica	1.09	(123)
121.3011	23.4016	15.95	0.39	K-Ar white mica	0.55	(123)
121.2729	23.2864	10.83	0.41	K-Ar white mica	0.82	(123)
121.2255	23.2885	5.55	0.49	K-Ar white mica	1.59	(123)
121.2471	23.3103	15.87	0.41	K-Ar white mica	0.56	(123)
121.1629	23.1315	25.71	0.6	K-Ar white mica	0.34	(123)
121.1658	23.1173	1.17	0.14	ZFT	6.70	(124)
121.2617	24.223	66.11	1.5	K-Ar white mica	0.13	(124)
121.2795	24.2236	75	1.7	K-Ar white mica	0.12	(124)
121.2884	24.2002	55.61	1.2	K-Ar white mica	0.16	(124)
121.2971	24.191	33	0.8	K-Ar white mica	0.27	(124)
121.2993	24.1863	27.1	0.6	K-Ar white mica	0.33	(124)
121.2834	24.1706	42.08	0.9	K-Ar white mica	0.21	(124)
121.3041	24.1828	22.36	0.5	K-Ar white mica	0.40	(124)
121.3103	24.1837	22.47	0.6	K-Ar white mica	0.39	(124)

Longitude	Latitude	Age* (My)	Error* (My)	System	Erosion rate [mm/year]	Ref.
121.3137	24.1844	16.5	0.4	K-Ar white mica	0.54	(124)
121.3164	24.1847	10.39	0.2	K-Ar white mica	0.85	(124)
121.3173	24.1886	11.69	0.3	K-Ar white mica	0.76	(124)
121.3199	24.1894	23.48	0.6	K-Ar white mica	0.38	(124)
121.3294	24.1873	13.11	0.4	K-Ar white mica	0.67	(124)
121.3368	24.1928	5.37	0.2	K-Ar white mica	1.64	(124)
121.3396	24.1909	4.75	0.3	K-Ar white mica	1.86	(124)
121.3431	24.1886	6.42	0.2	K-Ar white mica	1.38	(124)
121.3507	24.1833	4.64	0.2	K-Ar white mica	1.90	(124)
121.3608	24.1798	6.89	0.3	K-Ar white mica	1.28	(124)
121.3644	24.1796	4.31	0.8	K-Ar white mica	2.05	(124)
121.3865	24.185	7.08	0.8	K-Ar white mica	1.25	(124)
121.3762	24.197	4.6	0.5	K-Ar white mica	1.92	(124)
121.4141	24.2024	5.64	0.2	K-Ar white mica	1.57	(124)
121.4153	24.2129	4.32	0.3	K-Ar white mica	2.04	(124)
121.4561	24.2026	3.24	0.4	K-Ar white mica	2.73	(124)
121.4638	24.202	2.04	0.1	K-Ar white mica	4.33	(124)
121.4738	24.1961	1.92	0.2	K-Ar white mica	4.60	(124)
121.4895	24.185	1.51	0.2	K-Ar white mica	5.85	(124)
121.492	24.1819	1.2	0.4	K-Ar white mica	7.36	(124)
121.5116	24.1861	1.07	0.3	K-Ar white mica	8.26	(124)
121.1172	24.2327	2.51	0.1	K-Ar white mica	3.52	(124)
121.1753	24.2548	2.77	0.2	K-Ar white mica	3.19	(124)
121.1963	24.2517	4.52	0.1	K-Ar white mica	1.95	(124)
121.208	24.2578	5.95	0.2	K-Ar white mica	1.48	(124)
121.2106	24.2626	48.09	1.1	K-Ar white mica	0.18	(124)
121.2138	24.2497	50.89	1.2	K-Ar white mica	0.17	(124)
121.2201	24.2405	37.95	0.8	K-Ar white mica	0.23	(124)

Longitude	Latitude	Age* (My)	Error* (My)	System	Erosion rate [mm/year]	Ref.
121.2436	24.2544	49.57	1.1	K-Ar white mica	0.18	(124)
120.8214	23.2705	90.78	2	K-Ar white mica	0.10	(124)
120.8663	23.2805	37.13	0.8	K-Ar white mica	0.24	(124)
120.8887	23.2837	51.89	1.2	K-Ar white mica	0.17	(124)
120.906	23.2703	49.14	1.1	K-Ar white mica	0.18	(124)
120.9071	23.2617	17.31	0.4	K-Ar white mica	0.51	(124)
120.9178	23.2596	16.62	0.4	K-Ar white mica	0.53	(124)
120.9324	23.2634	6.59	0.2	K-Ar white mica	1.34	(124)
120.95	23.2686	12.54	0.3	K-Ar white mica	0.70	(124)
120.9584	23.2686	8.82	0.2	K-Ar white mica	1.00	(124)
120.9689	23.2641	4.01	0.5	K-Ar white mica	2.20	(124)
120.9728	23.2493	2.45	0.2	K-Ar white mica	3.61	(124)
120.986	23.2482	2.89	0.2	K-Ar white mica	3.06	(124)
121.0148	23.2099	2.24	0.3	K-Ar white mica	3.94	(124)
121.0195	23.1889	2.66	0.4	K-Ar white mica	3.32	(124)
121.034	23.1826	1.45	0.3	K-Ar white mica	6.09	(124)
121.0248	23.1714	1.15	0.1	K-Ar white mica	7.68	(124)
121.0439	23.1583	1.2	0.2	K-Ar white mica	7.36	(124)
121.0763	23.1394	1.05	0.2	K-Ar white mica	8.41	(124)
121.081	23.1389	1.03	0.2	K-Ar white mica	8.58	(124)
121.1023	23.1378	2.43	0.2	K-Ar white mica	3.64	(124)
121.1131	23.1339	1.33	0.3	K-Ar white mica	6.64	(124)
121.1309	23.1329	3.88	0.5	K-Ar white mica	2.28	(124)
121.1659	23.117	10.08	0.3	K-Ar white mica	0.88	(124)
121.1668	23.104	15.9	0.4	K-Ar white mica	0.56	(124)
121.515	24.1893	1.26	0.22	ZFT	6.22	(124)
121.5106	24.1848	0.76	0.11	ZFT	10.31	(124)
121.4888	24.1847	0.92	0.22	ZFT	8.51	(124)
121.4756	24.2176	0.89	0.2	ZFT	8.80	(124)
121.4763	24.2089	0.92	0.22	ZFT	8.51	(124)

Longitude	Latitude	Age* (My)	Error* (My)	System	Erosion rate [mm/year]	Ref.
121.4741	24.2	0.99	0.19	ZFT	7.91	(124)
121.474	24.1944	1.23	0.23	ZFT	6.37	(124)
121.4709	24.1978	1.08	0.18	ZFT	7.25	(124)
121.4541	24.201	1.38	0.21	ZFT	5.68	(124)
121.4356	24.1858	1.21	0.12	ZFT	6.47	(124)
121.4371	24.1827	1.38	0.21	ZFT	5.68	(124)
121.4158	24.2133	1.6	0.27	ZFT	4.90	(124)
121.4159	24.2069	3.14	0.44	ZFT	2.49	(124)
121.4122	24.1986	1.79	0.23	ZFT	4.38	(124)
121.4072	24.1945	1.19	0.15	ZFT	6.58	(124)
121.4098	24.1921	2.04	0.23	ZFT	3.84	(124)
121.4093	24.1886	2.56	0.38	ZFT	3.06	(124)
121.4061	24.1899	1.78	0.23	ZFT	4.40	(124)
121.4061	24.1899	1.56	0.23	ZFT	5.02	(124)
121.3999	24.1963	2.11	0.24	ZFT	3.71	(124)
121.3841	24.1971	1.12	0.22	ZFT	6.99	(124)
121.3752	24.1927	3.14	0.44	ZFT	2.49	(124)
121.3723	24.1933	2.63	0.36	ZFT	2.98	(124)
121.3723	24.1933	2.1	0.29	ZFT	3.73	(124)
121.3867	24.1849	2.2	0.31	ZFT	3.56	(124)
121.371	24.1758	1.56	0.21	ZFT	5.02	(124)
121.3626	24.1793	2.38	0.27	ZFT	3.29	(124)
121.3582	24.1819	2.64	0.2	ZFT	2.97	(124)
121.355	24.1828	2.18	0.27	ZFT	3.59	(124)
121.355	24.1828	1.97	0.21	ZFT	3.98	(124)
121.351	24.1822	1.74	0.34	ZFT	4.50	(124)
121.351	24.1822	2.22	0.18	ZFT	3.53	(124)
121.351	24.1822	1.79	0.38	ZFT	4.38	(124)
121.3491	24.1833	2	0.25	ZFT	3.92	(124)
121.3491	24.1833	2.02	0.13	ZFT	3.88	(124)
121.3491	24.1833	3.49	0.36	ZFT	2.24	(124)
121.3491	24.1833	1.83	0.12	ZFT	4.28	(124)
121.3491	24.1833	1.64	0.17	ZFT	4.78	(124)
121.3473	24.1849	1.58	0.37	ZFT	4.96	(124)
121.3452	24.1871	2.22	0.16	ZFT	3.53	(124)
121.3432	24.1887	2.46	0.59	ZFT	3.18	(124)
121.3432	24.1887	1.59	0.13	ZFT	4.93	(124)
121.3411	24.1902	2	0.14	ZFT	3.92	(124)
121.3411	24.1902	2.21	0.14	ZFT	3.54	(124)
121.3212	24.1895	2.87	0.23	ZFT	2.73	(124)
121.3118	24.1833	2.46	0.21	ZFT	3.18	(124)
121.3053	24.1826	4.6	0.3	ZFT	1.70	(124)

Longitude	Latitude	Age* (My)	Error* (My)	System	Erosion rate [mm/year]	Ref.
121.292	24.2001	35.1	1.5	ZFT	0.22	(124)
121.2615	24.2203	82.13	6.5	ZFT	0.10	(124)
121.282	24.167	30.21	2.15	ZFT	0.26	(124)
121.2633	24.134	30.5	1.5	ZFT	0.26	(124)
121.1578	23.1196	0.9	0.13	ZFT	8.70	(124)
121.1307	23.133	1.09	0.13	ZFT	7.19	(124)
121.0812	23.1392	0.82	0.12	ZFT	9.55	(124)
121.0758	23.1407	1.22	0.25	ZFT	6.42	(124)
121.0429	23.1589	0.82	0.16	ZFT	9.55	(124)
121.0268	23.1715	0.68	0.12	ZFT	11.52	(124)
121.0145	23.1768	1.53	0.19	ZFT	5.12	(124)
121.0126	23.1791	0.84	0.12	ZFT	9.33	(124)
121.0134	23.1844	1.02	0.15	ZFT	7.68	(124)
121.0329	23.177	0.99	0.18	ZFT	7.91	(124)
121.0337	23.1832	1.02	0.21	ZFT	7.68	(124)
121.0196	23.1895	1.07	0.14	ZFT	7.32	(124)
121.0111	23.1929	1.13	0.12	ZFT	6.93	(124)
121.0141	23.2112	1.04	0.14	ZFT	7.53	(124)
120.9605	23.2657	1.87	0.16	ZFT	4.19	(124)
120.9646	23.2727	2.23	0.19	ZFT	3.51	(124)
120.9505	23.2677	2.6	0.33	ZFT	3.01	(124)
120.9472	23.265	2.95	0.3	ZFT	2.66	(124)
120.9436	23.266	3.93	0.39	ZFT	1.99	(124)
120.9062	23.2692	38.32	3.61	ZFT	0.20	(124)
120.8977	23.2801	70.28	16.19	ZFT	0.11	(124)
120.8899	23.2873	47.25	6.49	ZFT	0.17	(124)
120.8798	23.2831	44.59	3.31	ZFT	0.18	(124)
120.8422	23.287	55.7	3.97	ZFT	0.14	(124)
121.2553	24.2181	80.44	5.51	ZFT	0.10	(124)
121.2418	24.2315	86.21	6.69	ZFT	0.09	(124)
121.244	24.2423	75.04	7.59	ZFT	0.10	(124)
121.0101	22.6479	59.7	3.9	ZFT	0.13	(125)
120.9518	22.5113	75.4	6.4	ZFT	0.10	(125)
120.8909	22.3773	54.4	6.1	ZFT	0.14	(125)
121.1755	23.1159	0.78	0.17	ZFT	10.04	(125)
121.0845	22.8983	2.26	0.34	ZFT	3.47	(125)
121.0494	22.7603	43.6	3.4	ZFT	0.18	(125)
121.3003	23.432	0.6	0.2	AFT	5.83	(125)
121.0666	22.9	0.7	0.2	AFT	5.00	(125)
121.0494	22.76	0.4	0.1	AFT	8.75	(125)
121.0167	22.65	0.7	0.3	AFT	5.00	(125)
120.8241	22.16121	1.69	0.36	AFT	2.07	(125)

Longitude	Latitude	Age* (My)	Error* (My)	System	Erosion rate [mm/year]	Ref.
121.515	24.025	0.859	0.15	AFT	4.07	(125)
121.0101	22.64799	0.918	0.349	AFT	3.81	(125)
120.9518	22.51132	1.17	0.37	AFT	2.99	(125)
120.8909	22.37738	2.26	0.66	AFT	1.55	(125)
120.8864	22.24932	2.35	0.43	AFT	1.49	(125)
120.9082	22.58925	0.388	0.174	AFT	9.02	(125)
120.8414	22.26861	1.6	0.34	AFT	2.19	(125)
120.7622	22.21603	1.83	0.56	AFT	1.91	(125)
120.8311	21.9565	27.9	2	AFT	0.13	(125)
120.8825	22.15458	2.26	0.38	AFT	1.55	(125)
120.7871	22.04087	3.95	1.42	AFT	0.89	(125)
120.7922	22.0336	5.49	1.2	AFT	0.64	(125)
St. Elias Range						
-143.503	60.4208	0.53	0.07	AHe	5.73	(126)
-143.542	60.3931	0.44	0.03	AHe	6.90	(126)
-143.504	60.4332	0.53	0.1	AHe	5.73	(126)
-143.7	60.3896	0.74	0.07	AHe	4.10	(126)
-143.764	60.8838	25.1	0.87	AHe	0.12	(126)
-143.417	60.5428	1.78	0.83	AHe	1.70	(126)
-143.976	60.2306	1.8	0.11	AHe	1.69	(126)
-143.79	60.6469	2.28	0.16	AHe	1.33	(126)
-143.725	60.4996	0.63	0.11	AHe	4.82	(126)
-143.724	60.6441	1.66	0.09	AHe	1.83	(126)
-140.53	60.1686	1.55	-	AHe	1.96	(126)
-140.348	60.1643	7.21	1.16	AHe	0.42	(126)
-140.461	60.2369	0.56	0.08	AHe	5.42	(126)
-143.984	60.4488	1.09	0.09	AHe	2.78	(126)
-140.712	60.1333	3.95	1.06	AHe	0.77	(126)
-144.315	60.9104	18.9	1.2	AHe	0.16	(126)
-144.377	60.694	10.7	1.31	AHe	0.28	(126)
-144.477	60.499	2.02	0.14	AHe	1.50	(126)
-141.158	60.2573	0.74	0.14	AHe	4.10	(126)
-142.544	60.7203	8.2	0.8	AHe	0.28	(127)
-142.356	60.2926	3.9	0.4	AHe	0.60	(127)
-143.117	60.3194	1.4	0.2	AHe	1.67	(127)
-143.312	60.2625	2.2	0.2	AHe	1.06	(127)
-141.176	60.1809	1	0.5	AHe	2.33	(127)
-142.415	60.6572	9.7	1	AHe	0.24	(127)
-142.415	60.7672	13.3	1.3	AHe	0.18	(127)
-142.637	60.7911	16	1.6	AHe	0.15	(127)
-142.534	60.6793	13	1.3	AHe	0.18	(127)

Longitude	Latitude	Age* (My)	Error* (My)	System	Erosion rate [mm/year]	Ref.
-141.117	60.2482	5.8	0.6	AHe	0.40	(127)
-144.205	61.3408	28.7	2.9	AHe	0.08	(127)
-144.19	51.3425	29.8	3	AHe	0.08	(127)
-144.141	61.3231	36.5	7.2	AHe	0.06	(127)
-144.152	61.3348	27.9	2.8	AHe	0.08	(127)
-142.401	60.9221	18.3	1.8	AHe	0.13	(127)
-141.158	60.2573	4.8	1.5	AHe	0.49	(127)
-141.454	60.2855	1.2	0.1	AHe	1.94	(127)
-141.764	60.3435	1.5	0.2	AHe	1.56	(127)
-142.544	60.7203	26	2.1	ZHe	0.23	(127)
-143.312	60.2625	47.7	7.6	ZHe	0.13	(127)
-141.08	60.1866	31.8	2.5	ZHe	0.19	(127)
-142.356	60.29255	0.7	0.11	AHe	3.33	(128)
-142.442	60.34337	0.58	0.04	AHe	4.02	(128)
-142.627	60.21338	1.79	0.59	AHe	1.30	(128)
-142.601	60.33398	0.91	0.04	AHe	2.56	(128)
-142.781	60.3026	1.02	0.17	AHe	2.29	(128)
-143.117	60.31937	1.47	0.43	AHe	1.59	(128)
-141.94	60.05915	1.96	0.54	AHe	1.19	(128)
-141.988	60.15477	2.86	0.52	AHe	0.82	(128)
-141.454	60.28552	0.71	0.025	AHe	3.29	(128)
-141.224	60.3095	1.34	0.18	AHe	1.74	(128)
-141.763	60.41838	1.96	-	AHe	1.19	(128)
-143.059	60.4608	0.76	0.07	AHe	3.07	(128)
-143.324	60.8622	22.8	1.8	AHe	0.10	(128)
-143.059	60.5608	0.72	0.1	AHe	3.24	(128)
-142.513	60.40072	0.85	0.07	AHe	2.74	(128)
-142.49	60.43331	0.81	0.03	AHe	2.88	(128)
-142.341	60.60122	6.86	1.26	AHe	0.34	(128)
-141.746	60.55415	9.03	0.5	AHe	0.26	(128)
-141.965	60.29503	0.68	0.08	AHe	3.43	(128)
-141.965	60.74383	16.9	1.15	AHe	0.14	(128)
-141.926	60.75363	20.7	1.2	AHe	0.11	(128)
-141.887	60.7601	27.8	2.79	AHe	0.08	(128)
-142.431	60.06517	2.98	0.77	AHe	0.78	(128)
-142.823	60.20113	1.04	0.03	AHe	2.24	(128)
-142.242	60.214	1.29	0.29	AHe	1.81	(128)
-143.503	60.4208	12.9	1.1	ZHe	0.47	(128)
-143.059	60.4608	5.1	1	ZHe	1.18	(128)
-143.059	60.4608	9.6	1.4	ZHe	0.63	(128)
-142.543	60.720	13.8	1.3	AFT	0.27	(129)
-142.358	60.293	5.5	1.6	AFT	0.67	(129)

Longitude	Latitude	Age* (My)	Error* (My)	System	Erosion rate [mm/year]	Ref.
-142.418	60.343	6.2	1.8	AFT	0.59	(129)
-142.627	60.213	6.3	1.2	AFT	0.58	(129)
-142.601	60.340	5.8	1.9	AFT	0.63	(129)
-143.312	60.263	4.0	1.1	AFT	0.92	(129)
-141.94	60.059	31.5	3.4	AFT	0.12	(129)
-141.176	60.181	5.7	1.8	AFT	0.64	(129)
-142.415	60.657	14.5	1.2	AFT	0.25	(129)
-142.606	60.767	27.3	2.5	AFT	0.13	(129)
-142.637	60.791	5.0	1.8	AFT	0.73	(129)
-142.534	60.679	13.3	1.2	AFT	0.28	(129)
-142.512	60.418	3.4	1.0	AFT	1.08	(129)
-141.080	60.186	28.7	3.5	AFT	0.13	(129)
-141.764	60.285	2.8	0.8	AFT	1.31	(129)
-142.544	60.720	34.4	1.7	ZFT	0.23	(129)
-142.627	60.213	39.6	1.6	ZFT	0.20	(129)
-142.601	60.334	44.8	2.0	ZFT	0.18	(129)
-141.940	60.059	33.8	2.0	ZFT	0.24	(129)
-142.637	60.791	48.4	2.4	ZFT	0.17	(129)
-142.512	60.418	31.4	1.4	ZFT	0.25	(129)
-141.080	60.187	34.0	1.5	ZFT	0.24	(129)
-141.764	60.285	37.3	1.5	ZFT	0.21	(129)
San Gabriel Mountains						
-118.017	34.16889	11.8	4	AFT	0.33	(26)
-118.218	34.2841	6.1	1.5	AFT	0.68	(26)
-118.185	34.2833	10	1.4	AFT	0.39	(26)
-118.051	34.218	11.9	1.3	AFT	0.32	(26)
-117.901	34.15139	5.3	0.5	AFT	0.80	(26)
-117.884	34.1675	3	1	AFT	1.54	(26)
-117.851	34.2	4.5	1.2	AFT	0.96	(26)
-117.668	34.20083	8.4	1.2	AFT	0.48	(26)
-117.801	34.2333	9	1.7	AFT	0.44	(26)
-117.784	34.21694	13	1.5	AFT	0.29	(26)
-117.635	34.28417	7	0.9	AFT	0.58	(26)
-117.852	34.20194	19.3	1.8	AFT	0.19	(26)
-117.767	34.26722	3.7	0.7	AFT	1.20	(26)
-117.85	34.25083	14.2	2.1	AFT	0.27	(26)
-118.152	34.28556	16.1	1.6	AFT	0.23	(26)
-118.017	34.16889	6.56	0.66	AHe	0.32	(26)
-118.185	34.2833	3.12	0.2	AHe	0.74	(26)
-118.051	34.218	7.59	0.46	AHe	0.27	(26)
-117.901	34.15139	6.27	0.62	AHe	0.34	(26)

Longitude	Latitude	Age* (My)	Error* (My)	System	Erosion rate [mm/year]	Ref.
-117.784	34.21694	6.79	0.41	AHe	0.31	(26)
-117.635	34.28417	5.12	0.31	AHe	0.42	(26)
-117.852	34.20194	8.86	2.44	AHe	0.23	(26)
-118.156	34.30595	5504.59	-	CRN [year]	0.11	(18)
-118.108	34.30622	5042.02	-	CRN	0.12	(18)
-118.121	34.31133	7142.86	-	CRN	0.08	(18)
-118.026	34.27808	17142.86	-	CRN	0.04	(18)
-118.12	34.33013	4444.44	-	CRN	0.14	(18)
-118.249	34.32839	2439.02	-	CRN	0.25	(18)
-118.148	34.29795	2371.54	-	CRN	0.25	(18)
-118.255	34.30291	1415.09	-	CRN	0.42	(18)
-118.196	34.28186	2150.54	-	CRN	0.28	(18)
-117.739	34.29655	726.39	-	CRN	0.83	(18)
-117.761	34.24197	594.06	-	CRN	1.01	(18)
-117.742	34.29671	1376.15	-	CRN	0.44	(18)
-118.021	34.2793	1910.82	-	CRN	0.31	(18)
-118.026	34.27816	2264.15	-	CRN	0.27	(18)
-118.049	34.35192	5555.55	-	CRN	0.11	(18)
-118.048	34.33878	3973.51	-	CRN	0.15	(18)
-118.08	34.21159	1290.32	-	CRN	0.47	(18)
-118.083	34.21833	1015.23	-	CRN	0.59	(18)
-118.085	34.21849	815.22	-	CRN	0.74	(18)
-118.01	34.33808	14285.71	-	CRN	0.04	(18)
-118.011	34.34042	12244.90	-	CRN	0.05	(18)
-117.99	34.38049	8219.18	-	CRN	0.07	(18)
-117.992	34.3659	6122.45	-	CRN	0.10	(18)
-117.99	34.36567	5660.38	-	CRN	0.11	(18)
-117.788	34.32853	4166.67	-	CRN	0.14	(18)
-117.889	34.2723	1015.23	-	CRN	0.59	(18)
-117.891	34.27165	1401.87	-	CRN	0.43	(18)
-117.95	34.24271	3174.60	-	CRN	0.19	(18)
-117.973	34.25391	2054.79	-	CRN	0.29	(18)
-118.027	34.28275	1857.59	-	CRN	0.32	(18)
-117.799	34.32044	1382.49	-	CRN	0.43	(18)
-117.801	34.32321	7594.94	-	CRN	0.08	(18)
-117.73	34.30563	542.50	-	CRN	1.11	(18)
-117.732	34.3058	577.48	-	CRN	1.04	(18)
-117.741	34.29591	836.82	-	CRN	0.72	(18)
-117.761	34.30274	596.42	-	CRN	1.01	(18)
-117.635	34.16493	2150.54	-	CRN	0.28	(18)
-117.635	34.16494	2752.29	-	CRN	0.22	(18)
-117.991	34.36052	972.45	-	CRN	0.62	(18)

Longitude	Latitude	Age* (My)	Error* (My)	System	Erosion rate [mm/year]	Ref.
-117.992	34.36191	5454.55	-	CRN	0.11	(18)
-117.791	34.23199	2166.06	-	CRN	0.28	(18)
-117.806	34.24076	2264.15	-	CRN	0.27	(18)
-117.992	34.36469	5042.02	-	CRN	0.12	(18)
-118.028	34.38171	7692.31	-	CRN	0.08	(18)
-118.102	34.30903	991.74	-	CRN	0.61	(18)
-117.9	34.3619	5084.75	-	CRN	0.12	(18)
-117.904	34.3598	6896.55	-	CRN	0.09	(18)
-117.965	34.3214	4081.63	-	CRN	0.15	(18)
-117.981	34.30427	2510.46	-	CRN	0.24	(18)

*All the thermochronological ages reported here are in My; however, the CRN ages are reported in year or ky indicated beside CRN in parentheses. In addition, the ages for CRN samples were computed by assuming the depth of erosion was 60 cm. Further, because these methods average erosional pulses from some time in past to the present, these ages are equal to the averaging time scale.

Sediment yield data were compiled from the following references: San Gabriel Mountains (24); central Himalayas (112); Taiwan (130). Decadal scale erosion rate for the Rhône valley reported here is from (93) for the sediment gauge that is at the mouth of the Rhône valley catchment. Decadal scale erosion rate for the St. Elias Range, Norway, Patagonia and Svalbard reported here are from (41) and (40). Estimated erosion rates for pacific NW are reported from (56). Millennial scale erosion rates for St. Elias range, Patagonia and Svalbard reported here were from (41, 127).